

# Lmx1a is required for the development of the ovarian stem cell niche in *Drosophila*

Andrew W. Allbee<sup>1</sup>, Diego E. Rincon-Limas<sup>2</sup> and Benoît Biteau<sup>1,\*</sup>

## ABSTRACT

The *Drosophila* ovary serves as a model for pioneering studies of stem cell niches, with defined cell types and signaling pathways supporting both germline and somatic stem cells. The establishment of the niche units begins during larval stages with the formation of terminal filament-cap structures; however, the genetics underlying their development remains largely unknown. Here, we show that the transcription factor Lmx1a is required for ovary morphogenesis. We found that Lmx1a is expressed in early ovarian somatic lineages and becomes progressively restricted to terminal filaments and cap cells. We show that Lmx1a is required for the formation of terminal filaments, during the larval-pupal transition. Finally, our data demonstrate that Lmx1a functions genetically downstream of Bric-à-Brac, and is crucial for the expression of key components of several conserved pathways essential to ovarian stem cell niche development. Importantly, expression of chicken Lmx1b is sufficient to rescue the null Lmx1a phenotype, indicating functional conservation across the animal kingdom. These results significantly expand our understanding of the mechanisms controlling stem cell niche development in the fly ovary.

**KEY WORDS:** Lmx1a, Stem cell niche, Ovary, *Drosophila*

## INTRODUCTION

*Drosophila* ovaries are composed of about 15-20 functional units called ovarioles that produce eggs. In each ovariole, somatic and germline stem cells are maintained by a group of specialized cells that form the niche (Eliazar and Buszczak, 2011; Kirilly and Xie, 2007). These niches are composed of terminal filaments (TFs) and cap cells, which provide signals required for the maintenance and function of the stem cell populations in adult ovaries, including BMPs and Hh (Eliazar and Buszczak, 2011; Kirilly and Xie, 2007). Although the origin of the somatic lineage in the female gonad has been established, the genetic factors underlying the morphogenetic processes required for the specification and establishment of TF-cap structures are largely unknown. Ovarian somatic cells originate from three mesoderm cell clusters on each side of the embryo (Boyle and DiNardo, 1995). During the mid-larval third instar (ML3), TF cells start to specify, expressing the TF marker Engrailed (En) (Bolívar et al., 2006; Gilboa, 2015). By late third larval instar (LL3), and continuing in white pre-pupae (WPP), TFs form well-organized stacks and promote the proliferation and migration of muscle

precursors that will develop into the muscular sheath and delimit individual ovarioles (Fig. S1A) (Irizarry and Stathopoulos, 2015). This process ensures that a single TF stack and a defined population of germline and somatic cells are incorporated in each unit.

The number of ovarioles and the developmental timing of the niche have been shown to be controlled by several signaling pathways, including Insulin, Hippo, Notch, Activin and Ecdysone pathways (Gancz and Gilboa, 2013; Gancz et al., 2011; Green and Extavour, 2014; Hodin and Riddiford, 1998; Lengil et al., 2015; Sarikaya and Extavour, 2015; Song et al., 2007). In addition, the two transcription factors Bab1 and Bab2, encoded by the *bric-à-brac* (*bab*) locus, are expressed in TFs and are essential for the formation of these structures (Couderc et al., 2002; Sahut-Barnola et al., 1995). Other BTB transcription factors, Pipsqueak, Trithorax-like and Batman (Lola like), also control TFs and ovariole numbers (Bartoletti et al., 2012). Finally, loss of the Engrailed transcription factor causes abnormal TF cell stacking (Bolívar et al., 2006). Although these signaling pathways and transcriptional regulators are essential for development of stem cell niches, the early genetic events coordinating TF-cap cell specification, formation and function remain largely unknown.

Here, we describe the expression and function of the LIM-homeodomain transcription factor Lmx1a in developing *Drosophila* ovaries. LIM-homeodomain proteins have essential roles during tissue patterning and cell differentiation in metazoans, from nematodes to vertebrates (Hobert and Westphal, 2000). Mammalian Lmx1a and Lmx1b are pleiotropic regulators of cell differentiation and tissue development in many organs, as shown by the defects and syndromes caused by loss-of-function mutations in these genes (Doucet-Beaupré et al., 2015). For instance, haploinsufficiency of Lmx1b causes nail-patella syndrome (NPS), a disorder affecting dorsal limb structures, kidneys, anterior eye components and the nervous system (Bongers et al., 2008; Dreyer et al., 1998; McIntosh et al., 1998; Vollrath et al., 1998). Studies in genetic mouse models have confirmed a regulatory function of Lmx1b in the development of these organs and the behavior of associated cell types, including serotonergic neurons, podocytes and several eye tissues (Burghardt et al., 2013; Chen et al., 1998; Ding et al., 2003; Miner et al., 2002; Morello et al., 2001; Pressman et al., 2000; Rohr et al., 2002). Similarly, studies of the mouse Lmx1a factor have revealed diverse developmental functions, including brain patterning and cell fate decision, dopaminergic neuron differentiation and insulin expression (Andersson et al., 2006; German et al., 1992). Finally, previous work has implicated Lmx1a and Lmx1b in a variety of other pathologies, including non-NPS renal disease (Edwards et al., 2015), Parkinson's disease (Laguna et al., 2015), and various forms of cancer, including ovarian epithelial carcinoma (He et al., 2014; Lin et al., 2012; Tsai et al., 2012; Tsai et al., 2013), highlighting the complexity of Lmx1a/b biology, as well as the urgent need to understand the function of these factors better.

<sup>1</sup>Department of Biomedical Genetics, University of Rochester Medical Center, 601 Elmwood Avenue, Rochester, NY 14642, USA. <sup>2</sup>Department of Neurology, McKnight Brain Institute, University of Florida, 1149 Newell Drive, FL 32611, USA.

\*Author for correspondence (benoit\_biteau@urmc.rochester.edu)

 B.B., 0000-0002-4850-4377

Two LIM-homeodomain proteins of the LMX subgroup are encoded in the *Drosophila* genome: *Lmx1a*/CG32105 and *Lmx1b*/CG4328. *Lmx1a* is expressed in the LL3 eye imaginal disc and its overexpression in this tissue causes eye defects (Roignant et al., 2010; Wang et al., 2016). However, the molecular, cell biological and developmental functions of this transcription factor have yet to be described. Here, we show that *Lmx1a* is expressed in somatic lineages in the developing ovary. We found that its expression becomes restricted to TFs and cap cells by LL3/P0 (freshly pupariated) and is maintained in the adult stem cell niche. Analyzing a CRISPR-generated *Lmx1a* knockout allele as well as cell type-specific and stage-specific knockdown of *Lmx1a*, we have determined that *Lmx1a* is required for ovary development specifically in the TF-cap cell niche at the time at which it forms. We performed transcriptional profiling of developing ovaries and placed *Lmx1a* downstream of *Bab1/2* in the specification of TF cells. We also show that without *Lmx1a*, several components of signaling pathways crucial to the forming niche are not properly expressed, including *Hh*, the transcription factors *Sox100B*, *Engrailed* and *Invected*, and confirmed that these genes are required in the *Lmx1a* lineage. Strikingly, expression of a chicken ortholog of *Lmx1a* in forming TF-cap cells is sufficient to rescue the *Lmx1a* null phenotype. We anticipate that these results will further elucidate the genetic and cell biological mechanisms underlying the establishment of the *Drosophila* ovary stem cell niche and provide insight into the role of LIM-HD factors in tissue development and patterning, homeostasis and disease.

## RESULTS

### ***Lmx1a* is expressed in developing and adult ovaries**

In a search for novel regulators of ovarian development in *Drosophila*, we found that the transcription factor *Lmx1a* is expressed in LL3 ovaries. Using RT-qPCR, we detected endogenous *Lmx1a* mRNA specifically in samples containing ovaries, compared with samples containing only fat body tissues (Fig. 1A). To confirm the specificity of the *Lmx1a* mRNA detection and to study its function, we generated a null allele, in which the CG32105 open reading frame is replaced by a 3xP3-DsRed cassette (*Lmx1a* $\Delta$ 1; Fig. S1B). Genome editing was validated by PCR amplification (Fig. S1C), and RT-qPCR confirmed that the *Lmx1a* transcript is undetectable in null animals, neither in adults nor in LL3 ovaries (Fig. 1A, Fig. S1D). Next, we took advantage of a reporter line in which the transcription factor *Gal4* is expressed under the control of a putative *Lmx1a* enhancer (*Lmx1a*-*Gal4*<sup>GMR42B09</sup>; Fig. S1B) to investigate the pattern and developmental history of *Lmx1a* expression in the ovary. When crossed individually with three RNAi lines against *Lmx1a* (Fig. S1B), *Lmx1a*-*Gal4* is sufficient to drive a loss of endogenous *Lmx1a* transcript in LL3/P0 transitioning ovaries comparable to *Lmx1a* mutant homozygotes, as detected by qPCR of cDNA generated from samples containing fat bodies and developing ovaries (Fig. 1B, Fig. S1E). This demonstrates that, at this stage, *Lmx1a* is exclusively expressed in all cells, or a subpopulation of cells, in which this driver is active. In P0 pupal ovaries, the *Lmx1a*-*Gal4* is active in apical cells, TFs and cap cells, as determined by morphology, colocalization with the TF marker *Engrailed*, and localization alongside the germline markers *Vasa* and  $\alpha$ -*Spectrin* (Fig. 1C,D, Fig. S1F). We also found that the dsRed transgene inserted in place of the *Lmx1a* coding sequence is strongly expressed in P0 TFs and cap cells and more weakly in apical cells (Fig. 1D, Fig. S1F), a pattern identical to that of *Lmx1a*-*Gal4*>UAS-

GFP and not observed in any other transgenic lines generated with the same 3xP3-DsRed cassette (data not shown).

We finally combined the *Lmx1a*-*Gal4* driver with the G-TRACE (*Gal4* technique for real-time and clonal expression) lineage-tracing system (Evans et al., 2009). GFP-based tracing suggests that *Lmx1a*-*Gal4* is active in the progenitors of all somatic cells (GFP), but its expression becomes restricted to the apical domain, which contains apical cells and TFs, by LL3 (RFP expression) (Fig. 1E). In adult ovaries, RFP expression suggests that this driver remains active only in the germline stem cell niche (TFs and cap cells), and GFP lineage tracing confirms that it is active earlier in the progenitors of follicle cells, follicle stem cells and muscle sheaths (Fig. 1F, GFP).

Together, these data strongly suggest that *Lmx1a* is expressed early during ovarian development, in the somatic progenitors. Its expression becomes limited to TFs and apical cells by LL3 and is further restricted to the germline stem cell niche in adult germaria.

### ***Lmx1a* is essential for ovary morphogenesis**

To begin addressing the function of *Lmx1a*, we analyzed phenotypes associated with *Lmx1a* mutation. Surprisingly, a close examination of homozygous null animals revealed no obvious morphological defects. Furthermore, homozygous adults were observed at the expected proportion in crosses between heterozygous animals, indicating no developmental delay or decreased fitness compared with control siblings (data not shown). However, analysis of fertility revealed that homozygous females are sterile and lay no eggs (Fig. 2A), whereas the fertility of males is not affected (Fig. S2A). In adult mutant females, ovaries are generally absent, with no significant amount of tissue attached to the oviducts (Fig. 2B). To confirm *Lmx1a* mutation as the cause of this phenotype, we generated trans-heterozygous animals carrying the *Lmx1a* $\Delta$ 1 knockout allele and several deletions covering the CG32105 locus. All mutant combinations result in viable adult females with absent ovaries (Fig. 2B). In a limited number of genetic backgrounds or at lower temperatures, residual mutant ovarian tissue can be recovered, presenting abnormal germaria and egg chambers and very few eggs attached to the oviducts or found dispersed in the abdominal cavity (Fig. S2B). The limited ovariole material appears highly disorganized, with egg chambers often fused together rather than separated and packaged by a muscular sheath. In the rare mutant germaria that could be recovered, we observed no morphologically recognizable TFs (Fig. S2B). This suggested to us that the development of muscle and TF-cap structures is aberrant in *Lmx1a* mutants.

Consistent with this, looking as early as in third instar larva, when TF morphogenesis starts to take place, we found evidence that ovarian development is aberrant. Based on morphology, cell organization and *Lmx1a*-dsRed expression, we found that although there is partial evidence of TF morphogenesis in *Lmx1a* $\Delta$ 1 homozygotes, these developing ovaries fail to generate the collection of fully formed, linear stacks early during the larval-pupal transition at LL3/P0 (Fig. 2C). By 24 or 48 h after pupariation, TFs are absent in mutant animals, the ovaries show no sign of growth and elongation, and primordial ovarioles do not form (Fig. 2D). To characterize these defects in more detail, we used well-established markers for TF-cap cells, *Engrailed* protein and *Bab1*<sup>P</sup>-*lacZ* reporter expression (Fig. 2E,F, Fig. S2C), as well as DE-cadherin (*Shotgun* in *Drosophila*) antibody staining to delineate their cellular boundaries (Fig. 2E) and collagen IV deposition around developing TFs (Fig. S2C; Van De Bor et al., 2015), in the ovaries of P0 heterozygous and null

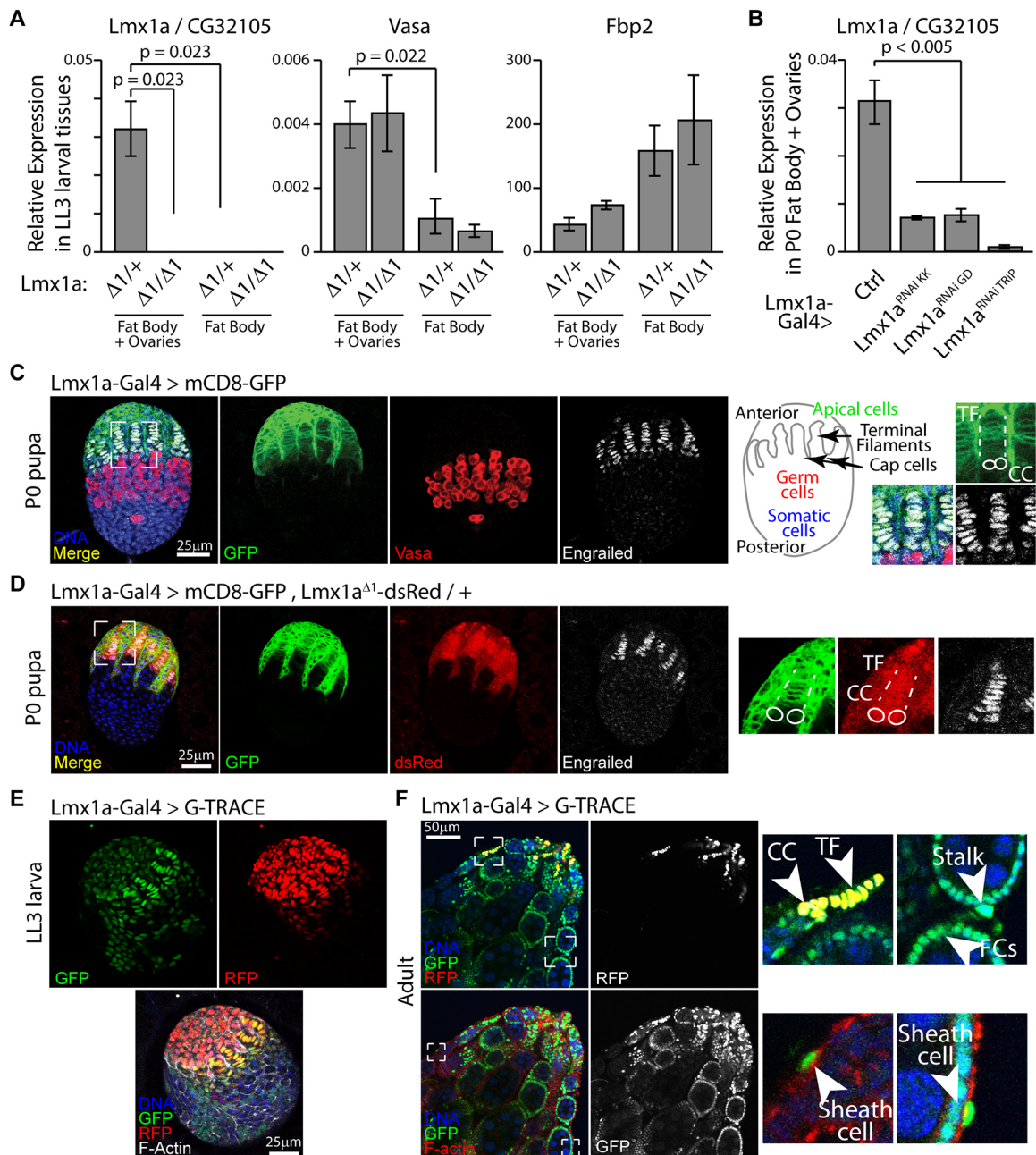


**Fig. 1. *Lmx1a* is expressed in developing and adult TFs, cap cells and sheath.** (A) qPCR analysis demonstrates that *Lmx1a* expression is specifically detected in samples containing LL3 ovaries, and not in samples containing exclusively fat body tissue. *vasa* and *Fbp2* expression are used to compare the relative amount of fat body and germline. The expression of all genes is normalized to *Actin 5C* expression. Values are presented as mean  $\pm$  s.e.m. of four biological replicates. *P*-values are calculated using two-tailed *t*-tests. (B) *Lmx1a* qPCR of P0 fat body tissue containing ovaries demonstrates three dsRNA constructs targeting different regions of the *Lmx1a* transcript are sufficient to nearly eliminate *Lmx1a* expression when driven in the *Lmx1a*-Gal4 domain. (C,D) Membrane-bound GFP driven by *Lmx1a*-Gal4<sup>GMR42B09</sup> marks TFs, apical cells and cap cells as determined by colocalization with Engrailed/Invected antibody staining, anterior location and adjacency to germline (*Vasa*-positive cells), respectively. Images on the right are magnifications of the boxed areas and reveal precise locations of TFs (dashed lines) and cap cells (ovals). The dsRed cassette used to replace the *Lmx1a* open reading frame and generate the *Lmx1a* <sup>$\Delta 1$</sup>  allele is expressed in a pattern precisely overlapping that of *Lmx1a*-Gal4<sup>GMR42B09</sup> (D). (E,F) Lineage-tracing analysis using the *Lmx1a*-Gal4<sup>GMR42B09</sup> driver combined with the G-TRACE system. RFP represents real-time activity, whereas GFP reports lineage labeling. *Lmx1a*-Gal4 is active in all pre-LL3 somatic cell types, becomes restricted to apical cells and TFs by LL3 (E) and TFs and cap cells in adults (F). Images on the right are magnifications of the boxed areas and reveal tracing to all adult somatic cell types (F). CC, cap cells; FCs, follicle cells.

animals. Our analysis shows that, although *Bab1*<sup>P-lacZ</sup>-positive cells are detected in *Lmx1a* <sup>$\Delta 1$</sup>  homozygotes, these cells fail to organize in individualized stacks with strong DE-cadherin staining (Fig. 2E,F), suggesting that these cells are initially specified but are not capable of proceeding normally through

differentiation. Confirming this notion, we found that none of these cells shows the strong Engrailed expression characteristic of TFs and cap cells in P0 ovaries (Fig. 2E). Finally, these aberrant TFs do not support collagen IV deposition like control structures do (Fig. S2C).

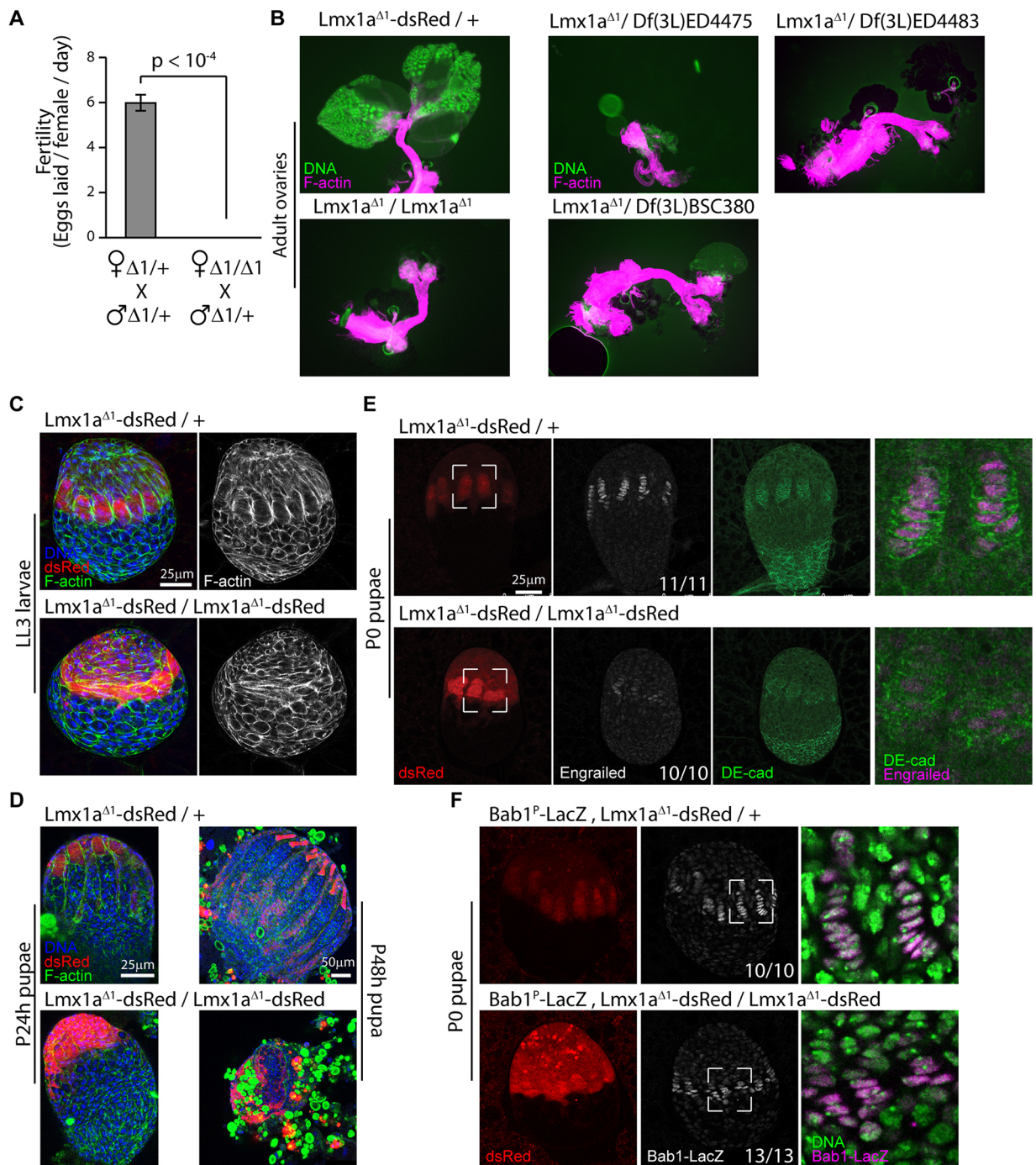


**Fig. 2. *Lmx1a* is required for ovary organogenesis.** (A) Fertility assay demonstrating that *Lmx1a* homozygous mutant females do not lay eggs. Five cohorts of four females were analyzed per genotype. Values are presented as mean  $\pm$  s.e.m. *P*-value was calculated using a two-tailed *t*-test. (B) Homozygous *Lmx1a* mutants display a near-complete loss of ovariole material in adult animals, whereas heterozygotes display normal morphology. Transheterozygotes for *Lmx1a* $^{\Delta 1}$  and any of three deficiency alleles that span the *Lmx1a* locus show a similar loss of ovaries in adult females. (C,D) Representative images comparing *Lmx1a* $^{\Delta 1}$  homozygous versus heterozygous ovaries throughout development. (C) Homozygotes show loss of TF stacking and absence of apical cell migration in LL3 (C) and early pupae (p24h; D), as shown by the lack of stacking of dsRed-positive cells delimited by cell-cell interfaces stained by phalloidin (F-actin). By mid-metamorphosis (P48h), severe ovary dysgenesis is apparent. (E) Expression of the TF-specific marker Engrailed is substantially reduced and DE-cad cell boundary staining reveals TF stacking defects in *Lmx1a* $^{\Delta 1}$  homozygotes. For both genotypes, the proportion of ovaries displaying either normal or reduced Engrailed/Invected staining is indicated. (F) Activity of the TF marker Bab1<sup>P</sup>-lacZ  $\beta$ -galactosidase antibody staining intensity is not reduced in *Lmx1a* $^{\Delta 1}$  homozygotes, but the staining pattern reveals TF stacking and elongation defects. Panels on the right are magnifications of the boxed areas. For both genotypes, the proportion of ovaries displaying normal levels of  $\beta$ -galactosidase antibody staining is indicated.

Altogether, these data demonstrate that *Lmx1a* is required for ovarian development and, in particular, the normal differentiation of TFs.

***Lmx1a* is required in TFs during the larval-pupal transition**  
Based on the expression pattern of *Lmx1a* in the developing ovary and the defect caused by its mutation, we hypothesized that *Lmx1a*

is required in TFs for their differentiation, formation and/or developmental function as organizing centers for niche establishment and ovariole morphogenesis. To test this notion, we first used *Lmx1a*-Gal4 to rescue *Lmx1a* expression in *Lmx1a* null animals. We found that expressing an HA-tagged version of the protein significantly restores overall ovary morphogenesis, including sheath development, TF formation and egg laying (Fig. 3A, Fig. S3A,B). In order to test the functional conservation between *Drosophila* *Lmx1a* and *Lmx1a/b* in vertebrates, we drove expression of chicken *Lmx1b* with *Lmx1a*-Gal4 and observed a significant rescue of the null mutant phenotype, comparable to that achieved by the *Lmx1a*-HA construct in terms of both overall morphology and fertility (Fig. 3A, Fig. S3B; UAS-c*Lmx1b*). Of note, the rescue by both *Drosophila* *Lmx1a* and chicken *Lmx1b* expression in TFs is much more pronounced at a lower temperature, at which development is slower (compare phenotypes at 18°C in Fig. 3A with 25°C in Fig. S3B).

In a set of converse experiments, we used the same driver to express several distinct dsRNA constructs targeting the *Lmx1a* transcript and knocking down its expression in TFs and apical cells in an otherwise wild-type organism (Fig. 1B, Fig. S4). Consistent with the requirement for *Lmx1a* in TFs, these manipulations strongly impair ovary development and female fertility, much like null homozygotes (Fig. 3B,D). Interestingly, we identified another Gal4 reporter, driven by a distinct putative *Lmx1b/a* enhancer (*Lmx1b*-Gal4<sup>GMR35G09</sup>; Fig. S1B), which is also active early in somatic lineages, as shown by lineage tracing, and remains active in P0 apical cells but is not active in P0 TF-cap structures (Fig. S4). Using this driver to knock down the expression of *Lmx1a*, we did not observe strong ovarian defects: only a mild phenotype with one of the RNAi lines (KK) and no significant phenotype with the other (TRiP) (Fig. 3C). This correlates with a complete loss of egg laying when driving expression of *Lmx1a*<sup>RNAi(TRiP)</sup> with the *Lmx1a*-Gal4 driver (active in LL3-P0 TF-cap cells) and normal fertility when expression of the same construct is driven by *Lmx1b*-Gal4<sup>GMR35G09</sup> (not active in LL3-P0 TF-cap cells; Fig. 3D). This strongly suggests that *Lmx1a* is essential in TFs and cap cells themselves, with a minimal role in apical cells, to support ovarian development.

To confirm these findings, we took advantage of additional drivers active in developing ovaries. The *bric-à-brac* (*bab*) locus encodes two transcription factors, *Bab1* and *Bab2*, expressed in apical cells and developing TFs and is essential for ovary development (Couderc et al., 2002; Godt and Laski, 1995; Sahut-Barnola et al., 1995). The *bab1*-Gal4 drivers are highly active in P0 TFs (Cabrera et al., 2002) (Fig. 3B, Fig. S4). The strong ovarian defects observed in *bab1*-Gal4>*Lmx1a* RNAi animals, which recapitulate the *Lmx1a* mutant phenotype, thus confirm that *Lmx1a* is required in TFs to support ovarian morphogenesis (Fig. 3B, Fig. S5). In addition, a previous study showed that components of the FGF signaling pathway, *thisbe* (*ths*, FGF-like ligand) and *heartless* (*htl*, FGF receptor), are expressed in TFs and apical cells, respectively (Irizarry and Stathopoulos, 2015). Therefore, we also used *ths*-Gal4 and *htl*-Gal4 to reduce the expression of *Lmx1a* in these cells (Fig. S5). G-TRACE analysis confirmed that *htl*-Gal4 activity is restricted to the apical cells in P0 ovaries and showed that *ths*-Gal4, although active in all TF cells by adulthood (data not shown), drove RFP expression in only a few TF cells at P0 (Fig. S4). Consistent with our model, we found that *Lmx1a* RNAi expression, using these two drivers, does not affect the development of ovaries. Interestingly, in their study, Irizarry and Stathopoulos demonstrate that TFs are essential for the proliferation of apical cells and proper development of the sheaths (Irizarry and

Stathopoulos, 2015). This, combined with our results, strongly suggests that *Lmx1a* is required for TF differentiation and/or developmental function, and that the absence of muscle sheaths in *Lmx1a* mutants is a consequence of TF defects.

Finally, to establish the temporal requirement of *Lmx1a* in TFs, we conducted a series of temperature-sensitive knockdown and rescue experiments using the *Lmx1a*-Gal4 driver combined with the temperature-sensitive *tub*-Gal80<sup>ts</sup> inhibitor. We found that *Lmx1a* RNAi expression starting in mid-stage L3 larvae (ML3, around 24 h before pupariation when animals are switched to 29°C) is sufficient to cause severe ovarian defects and recapitulate the ovary phenotype observed when *Lmx1a* expression is knocked down throughout development (Fig. 4A). In contrast, *Lmx1a* RNAi expression 24 h after pupariation does not cause any significant defect. Conversely, re-expressing *Lmx1a* in the null background starting in ML3 rescues the ovarian mutant phenotype, just as much as re-expressing the transgene throughout development, and re-expression starting 24 h after pupariation does not visibly ameliorate ovarian development (Fig. 4B). These results define a developmental window of about 48 h around the larval-pupal transition during which *Lmx1a* is required for ovary morphogenesis.

Altogether, our data demonstrate that, although *Lmx1a* is potentially expressed in very early common somatic progenitors and its expression is maintained into adulthood, it is required specifically in TFs during a critical developmental window, the larval-pupal transition, for the proper differentiation of these cells and normal development of the ovary.

### ***Lmx1a* controls a large developmental program in the developing ovary**

The morphogenetic mechanisms that control the establishment of individual ovarioles and overall *Drosophila* ovary development are beginning to be elucidated. For example, Hedgehog, Notch, FGF, Insulin and Hippo signaling pathways control the specification and number of TF stacks and cap cells that in turn coordinate the development of each ovariole (Forbes et al., 1996; Gancz and Gilboa, 2013; Green and Extavour, 2014; Irizarry and Stathopoulos, 2015; Sarikaya and Extavour, 2015; Song et al., 2007). However, the sequence of signaling events and transcriptional cascade(s) required for the development of these structures are still largely unclear. Because *Lmx1a* is required specifically in developing TF-cap structures, we hypothesized that *Lmx1a* is, in turn, essential for many crucial niche-forming developmental pathways, which would explain the near complete loss of ovary material by adulthood in *Lmx1a* null animals. To test this notion, we analyzed the transcriptomes of LL3/P0 developing ovaries embedded in fat body tissue compared with surrounding fat body alone, and compared *Lmx1a* null tissues with heterozygous controls.

We first generated a list of genes that are significantly enriched in ovary-containing samples. Among these genes, we identified many transcripts of proteins known to be expressed in developing *Drosophila* ovaries (e.g. *Vasa*, Hedgehog, *Wnt4*, *Bab1*, *Bab2*, *Engrailed*, *Invected* and *Sox100B*) (Fig. 5A,C), confirming the specificity of our methodology. Within this list of 1755 genes enriched in ovaries, we then compared *Lmx1a*<sup>Δ1</sup> homozygotes with heterozygotes in order to identify the genes most highly affected by the loss of *Lmx1a*. Strikingly, we found components of the Hedgehog, Notch and FGF pathways (*hh* and *ptc*, *Ser*, and *stumps*, respectively) in addition to *engrailed*, *invected* and *Sox100B* among the 48 reduced transcripts in *Lmx1a* null developing ovaries (Fig. 5B,C; Table S1), suggesting that these genes are direct or

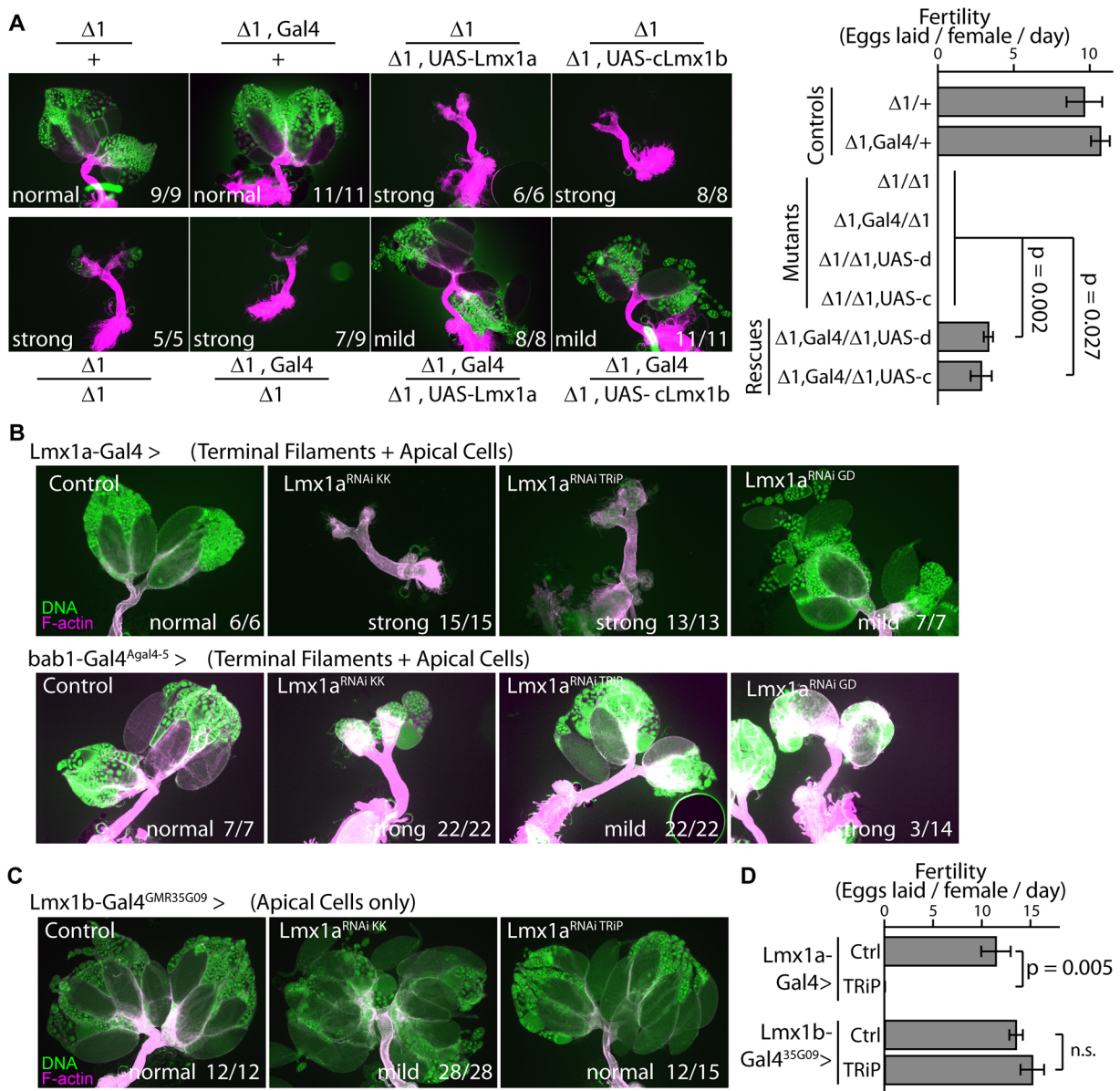


**Fig. 3. Lmx1a is required in TFs for their development.** (A) Both UAS-Lmx1a and UAS-cLmx1b, driven by Lmx1a-Gal4, are sufficient to rescue the *Lmx1a* <sup>$\Delta 1$</sup>  homozygous background. Rescue is apparent in terms of overall ovariole material, sheath (stained with phalloidin) and fertility. Three to four cohorts of four females were analyzed per genotype. Values are presented as mean  $\pm$  s.e.m. and *P*-values were calculated using two-tailed *t*-tests comparing rescue genotype fertility with their corresponding mutant controls. (B,C) Three Lmx1a<sup>RNAi</sup> lines, each targeting different regions of the transcript, recapitulate the Lmx1a null phenotype when driven by drivers that express in both TF-cap structures and apical cells: Lmx1a-Gal4 and bab1-Gal4<sup>Gal4-5</sup> (see Fig. S4 for activity patterns in the ovaries of P0 animals). Expression of Lmx1a<sup>RNAi</sup> constructs using Lmx1b-Gal4<sup>GMR35G09</sup>, a driver that expresses in apical cells but not TF-caps in P0 ovaries, does not induce ovary defects. (D) Lmx1a<sup>RNAi</sup>, when driven by Lmx1a-Gal4 but not Lmx1b-Gal4<sup>GMR35G09</sup>, causes a complete loss of fertility. Three to four cohorts of four females were analyzed per genotype. Values are presented as mean  $\pm$  s.e.m. and *P*-values were calculated using two-tailed *t*-tests comparing Lmx1a<sup>RNAi</sup>-expressing conditions with corresponding controls. For each condition, the severity of the phenotype and the proportion of abnormal ovary pairs observed are indicated. n.s., not significant.

indirect targets of Lmx1a. Conversely, we found that other factors essential for ovary development and mentioned before, such as Bab1, Bab2, Wnt4, Ths and Htl, are not affected in Lmx1a mutants (Fig. 5C), raising the possibility that these factors are regulated upstream of or in parallel to Lmx1a.

To validate these results, we performed qPCR on cDNA generated from the same samples and found no change in *vasa*, *bab1* and *bab2* transcript levels and confirmed a significant reduction in *hh* and *Ser* transcript levels in Lmx1a homozygous mutants (Fig. 5D).

### Lmx1a functions genetically downstream of Bric-à-Brac

Prior to this study, the *bab1/2* locus was one of the only loci known to be essential cell-autonomously in forming TF-cap niche structures (Bolívar et al., 2006; Couderc et al., 2002). The maintenance of Bab1 and Bab2 expression in *Lmx1a* <sup>$\Delta 1$</sup>  homozygotes, as revealed through RNAseq, qPCR (Fig. 5B,C,D) and the Bab1<sup>P-lacZ</sup> reporter (Fig. 2F), suggested to us that Lmx1a may function downstream of Bab1/2. Further confirming that Lmx1a is not required for Bab1 expression, we found that knockdown of Lmx1a, although inducing morphologically

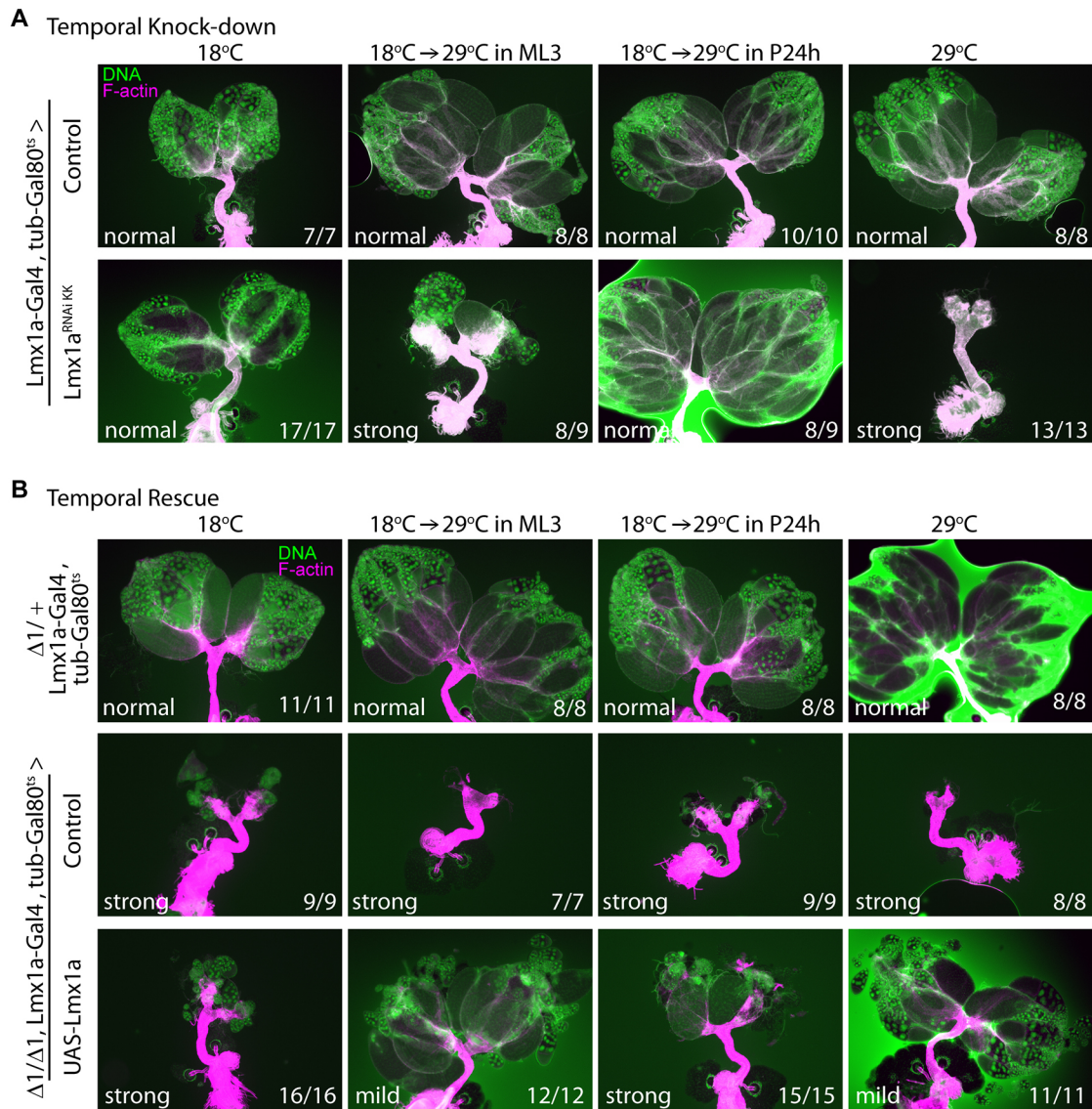


**Fig. 4. Lmx1a is required during the larval-pupal transition.** Temporal knockdown and rescue of Lmx1a expression in developing ovaries. The Lmx1a-Gal4 driver was combined with the tub-Gal80<sup>ts</sup> repressor to control transgene expression by shifting developing animals from 18°C to 29°C. Representative images of adult ovary phenotypes of animals placed at restrictive temperatures at the indicated developmental time points are presented. (A) Lmx1a<sup>RNAi</sup>-mediated ovary phenotype only occurs when Lmx1a-Gal4 is active at the LL3/P0 transition. (B) UAS-Lmx1a-HA-mediated rescue of Lmx1a $\Delta 1$  homozygous ovary defects only occurs when Lmx1a-Gal4 is active at the same developmental transition. For each condition, the severity of the phenotype and the number of ovary pairs observed are indicated.

defective TFs, did not affect *Bab1<sup>P</sup>-lacZ* reporter activity (Fig. 6A). We next investigated whether *Bab1/2* and *Lmx1a* function in the same lineage. Consistent with this notion, we found that expression of RNAi against either *bab1* or *bab2* in the *Lmx1a* lineage, using the *Lmx1a*-Gal4 driver, induces an ovary defect comparable to that previously reported in *Bab1/2* mutant homozygotes, with substantially reduced, disorganized and fused ovariole material (Couderc et al., 2002), and is comparable to what we observe in *Lmx1a* mutants or *Lmx1a*-Gal4>*Lmx1a*RNAi animals (Fig. 6B). This raised the possibility that *Bab1/2* is essential for *Lmx1a* expression and function. To test this hypothesis, we analyzed the endogenous level of *Lmx1a* mRNA in *bab1<sup>P</sup>/bab1<sup>P</sup>* homozygous ovaries. It has been previously reported that the *Bab1<sup>P</sup>-lacZ* insertion causes a mutation in *Bab1*, but not *Bab2*, and homozygous mutants show a severe ovary defect (Couderc et al., 2002). In P0 ovaries of these mutants, we show that *Lmx1a*

expression is very significantly reduced compared with samples dissected from heterozygous siblings (Fig. 6C), placing *Bab1* genetically or temporally upstream of *Lmx1a* in the development of the TF-cap structure.

#### Multiple Lmx1a-dependent genes are required for ovary development

We next functionally validated a collection of genes identified as being dysregulated in *Lmx1a* mutants. To this end, we drove the expression of RNAi constructs directed against *Hh*, *Sox100B*, *Engrailed* and *Invected* in the *Lmx1a*-Gal4 lineage in a control background or in a *Bab1* heterozygous sensitized background (*Bab1<sup>P</sup>-lacZ/+*). Consistent with the known crucial role for *Hh* in the function of the ovarian stem cell niche (Forbes et al., 1996), we found that the expression of *Hh* dsRNA within the *Lmx1a*-Gal4 lineage induces a strong loss of fertility and a defect in ovary

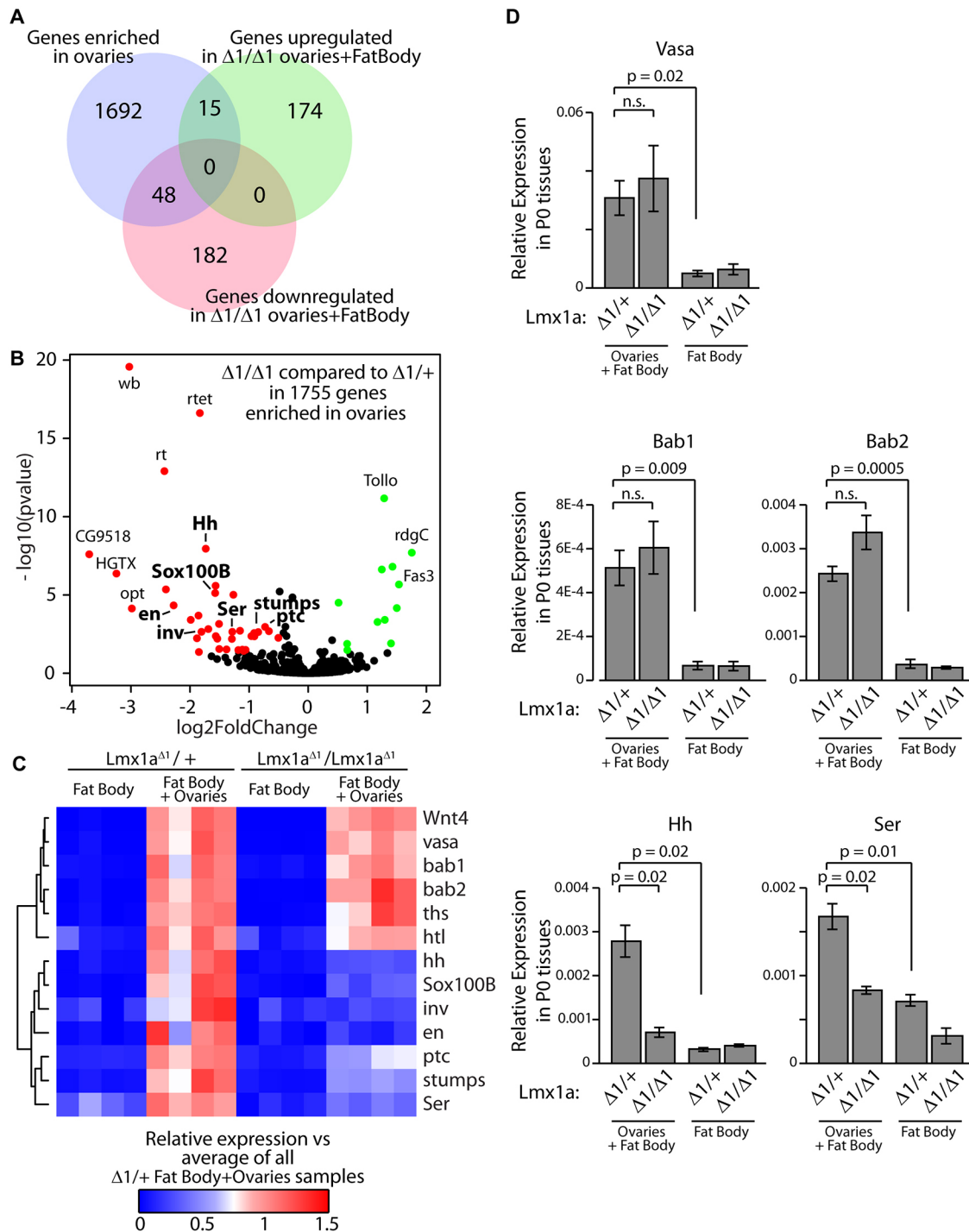


**Fig. 5. *Lmx1a* is essential for the expression of genes and components of signaling pathways known to be involved in the ovarian niche.** (A) Venn diagram displaying the number of genes enriched in ovaries compared with fat body that are either increased or decreased in *Lmx1a* <sup>$\Delta 1$</sup>  homozygotes relative to heterozygotes. (B) Volcano plot displaying transcripts that are significantly upregulated (green) or downregulated (red) in *Lmx1a* <sup>$\Delta 1$</sup>  homozygotes compared with heterozygotes according to adjusted *P*-value (<0.05) and fold change ( $\log_2\text{FoldChange} > 0.5$  or  $< -0.5$ ). Components of pathways known to be necessary for niche formation and/or function are labeled in bold. (C) Heat map demonstrating the enrichment of germline and stem cell niche factors in fat body samples containing ovaries, and the loss of several of these factors in *Lmx1a* <sup>$\Delta 1$</sup>  homozygotes compared with heterozygotes. (D) Validation of RNAseq data by qPCR. *vasa*, *bab1*, *bab2*, *hh* and *Ser* transcripts are all enriched in samples containing ovaries. *vasa*, *bab1* and *bab2* remain unchanged whereas *hh* and *Ser* are significantly reduced in *Lmx1a* <sup>$\Delta 1$</sup>  homozygotes. Values are presented as mean  $\pm$  s.e.m. of four biological replicates. *P*-values were calculated using two-tailed *t*-tests. n.s., not significant.

morphogenesis, which is enhanced by *Bab1*<sup>*lacZ*</sup> heterozygosity (Fig. 7). Next, although *Sox100B* has been reported to be expressed in TFs of developing ovaries, no role for this protein in ovary

morphogenesis has been detected, potentially due to the failure of *Sox100B* mutant flies to fully emerge and produce mature ovaries suitable for proper assessment of adult phenotype (Nanda et al.,



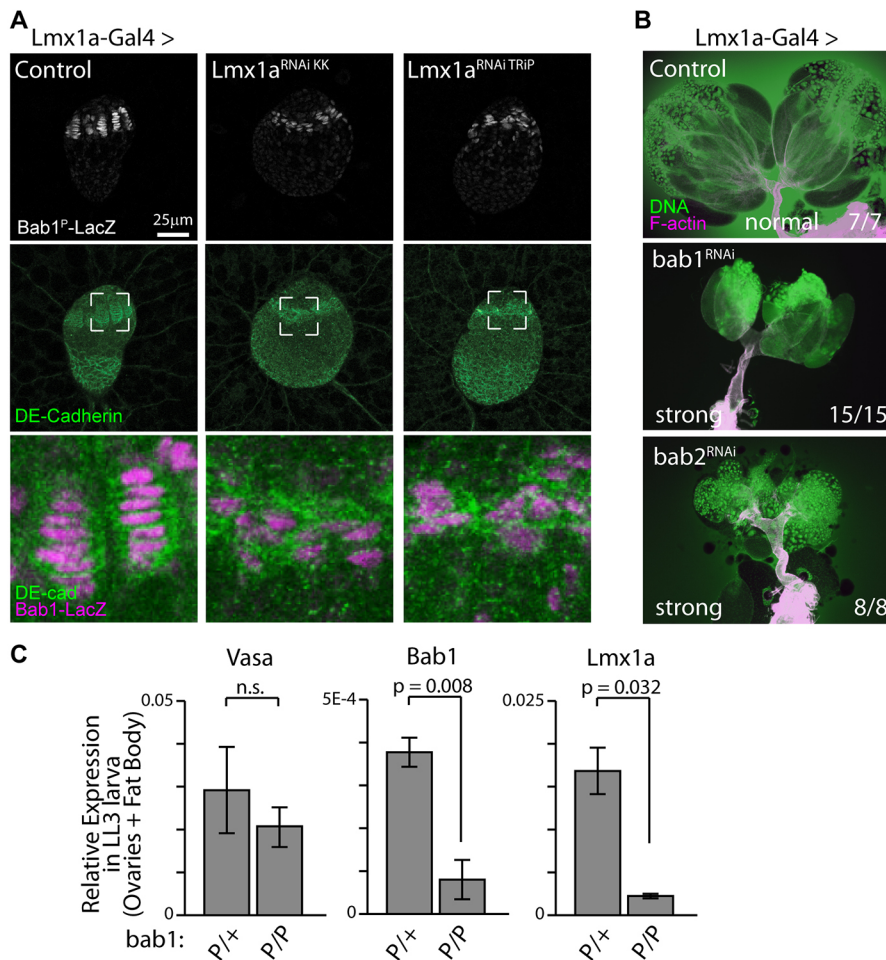


**Fig. 6. Lmx1a functions downstream of Bric-à-Brac.** (A) Knockdown of Lmx1a by RNAi driven by Lmx1a-Gal4 is sufficient to induce defects in TF stacking but does not affect Bab1<sup>P</sup>-LacZ staining intensity. (B) RNAi-mediated Bab1 and Bab2 knockdown driven by Lmx1a-Gal4 is sufficient to induce strong ovary developmental defects. (C) qPCR analysis of LL3/P0 animals homozygous for the Bab1<sup>P</sup>-LacZ null allele demonstrates substantial loss of Lmx1a transcript compared with heterozygotes. bab1 expression is lost and vasa expression unchanged, as expected. For each condition, the severity of the phenotype and the proportion of abnormal ovary pairs observed are indicated in B. Values are presented as mean±s.e.m. of three biological replicates. P-values were calculated using two-tailed t-tests. n.s., not significant.

2009). Driving the expression of Sox100B dsRNA within the Lmx1a-Gal4 lineage resulted in a mild ovary defect, and reduced fertility when combined with Bab1 heterozygosity (Fig. 7), suggesting a developmental role for Sox100B within the Lmx1a-Gal4 lineage. Finally, Engrailed has been suggested to be required for proper stacking of TF cells (Bolívar et al., 2006), and is essential for *decapentaplegic* (*dpp*) expression in cap cells, a crucial niche signal maintaining germline stem cell self-renewal (Eliazar et al., 2014; Luo et al., 2017; Rojas-Ríos et al., 2012; Xie and Spradling, 1998). Because of the possibility of redundancy between Engrailed and Invected, which are both affected in Lmx1a mutants, we simultaneously drove En<sup>RNAi</sup> and Inv<sup>RNAi</sup> in the Lmx1a-Gal4 lineage. In these strong knockdown conditions (Fig. S6), we found that the combined loss of Engrailed and Invected produces a mild phenotype in young animals comparable to that of Lmx1a-Gal4>Sox100B RNAi animals and slightly reduced fertility in control background (Fig. 7A,C). However, consistent with the known role for Engrailed in adult niche maintenance (Luo et al., 2017), we observed strong ovarian defects in older females (11 days old). Furthermore, we observed a complete loss of ovary morphogenesis and fertility in En/Inv knockdown animals carrying the Bab1<sup>P</sup>-LacZ allele (Fig. 7B,C). This confirms that, in addition to its role in the adult niche, Engrailed, along with Invected, plays at least a partial role in the Lmx1a lineage for ovary development.

Based on its amino acid sequence, especially the predicted LIM and homeobox domains, it is very likely that Lmx1a functions as a transcription factor. In order to function, LIM-HD factors often

require the co-factor Ldb (LIM domain binding) to mediate either homo- or heterodimer interactions. In support of this, Wang et al. found that Lmx1a requires the co-factor Chip (the known *Drosophila* Ldb homolog) to mediate eye developmental defects when expressed ectopically in the LL3 eye imaginal disc (Wang et al., 2016). We reasoned that Lmx1a might require Chip to mediate its function in the developing ovary and found that Chip<sup>RNAi</sup> expression, using the Lmx1a-Gal4 driver, produces ovary developmental defects similar to Lmx1a mutants (Fig. S7). Previous studies on several LIM-HD factors suggest that Chip mediates the formation of either homodimers or heterodimers with other LIM-HD factors (Hobert and Westphal, 2000; Roignant et al., 2010; Wang et al., 2016). Further studies will be required to determine whether Lmx1a interacts with another LIM-HD factor to regulate TF-cap development and function.

Altogether, our genetic analyses demonstrate that multiple Lmx1a-dependent genes are required in the Lmx1a-Gal4 lineage for ovary morphogenesis. This, combined with our RNAseq analysis, supports a model in which Lmx1a functions upstream of a collection of signaling and transcriptional events essential for the differentiation of TF-cap cells, stem cell niche establishment/maintenance and, consequently, ovary morphogenesis. Additional studies will be required to investigate whether Lmx1a directly and transcriptionally controls the expression of these genes in TF-cap cells.

## DISCUSSION

Despite longstanding interest in the *Drosophila* ovary as a model for the adult stem cell niche, the genetic mechanisms underlying

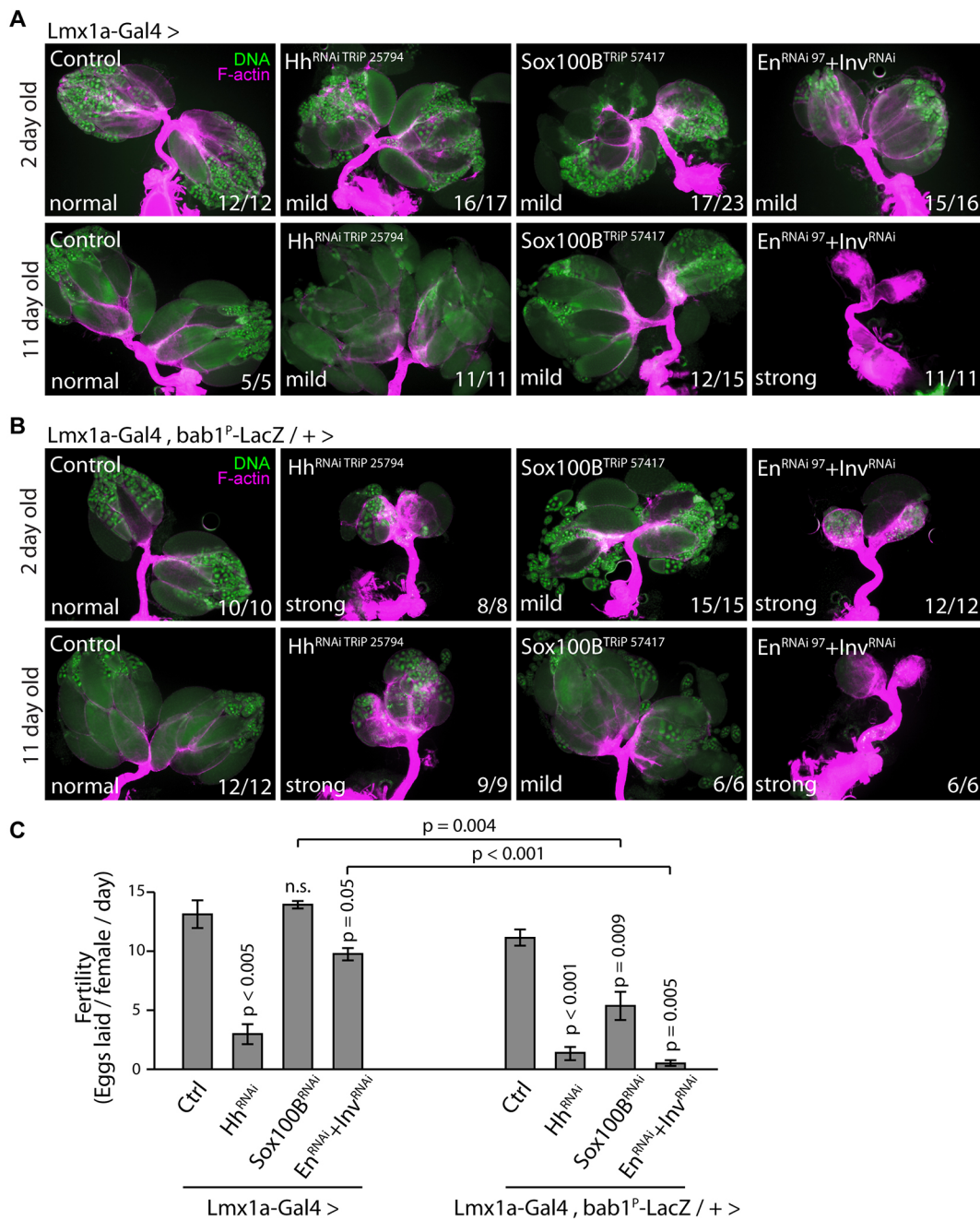


**Fig. 7. Functional analysis of genes downstream of Lmx1a.** (A) Expression of dsRNA constructs against Hh, Sox100B and simultaneously Engrailed and Invested, driven by Lmx1a-Gal4, induces mild ovary defects by early adulthood (2 days old). The defect observed with simultaneous Engrailed and Invested dsRNA expression is enhanced with age (11-day-old females). (B) Identical knockdown experiments performed in a Bab1<sup>P</sup>-lacZ heterozygous background induces a stronger phenotype with Hh<sup>RNAi</sup> and simultaneous En<sup>RNAi</sup>+Inv<sup>RNAi</sup> expression. (C) Female fertility under the same genetic conditions: Expression Hh<sup>RNAi</sup> or simultaneous En<sup>RNAi</sup>+Inv<sup>RNAi</sup>, in the Lmx1a-Gal4 lineage, causes a loss of fertility. Bab1<sup>P</sup>-lacZ heterozygous background enhances the loss of fertility observed with En<sup>RNAi</sup>+Inv<sup>RNAi</sup>. Sox100B dsRNA expression, in this background, reduces fertility. Four cohorts of four females were analyzed per genotype. Values are presented as mean±s.e.m. and P-values were calculated using two-tailed t-tests and compared with the control cross when the same driver was used, or between drivers when comparing fertility for the same RNAi construct. n.s., not significant.

the initial establishment and development of the niche remain largely unexplored. To date, only two transcription factor loci, *bric-à-brac* and *engrailed/invested*, have been identified as required for the development or proper stacking of TFs, and their function remains largely unknown (Bolívar et al., 2006; Godt and Laski, 1995). In this study, we characterized the function of Lmx1a, a highly conserved LIM homeobox transcription factor, in the developing *Drosophila* ovary. By generating an *Lmx1a*

knockout line as well as taking advantage of a novel collection of Gal4 drivers that produce spatially restricted developing ovary expression patterns, we show that Lmx1a is required in TF-cap structures at the time at which they form and initiate ovarian stem cell niche establishment and ovariole morphogenesis. It remains unclear whether Lmx1a plays a role in TFs, cap cells, or both. Our data also suggest that Lmx1a expression is maintained in the adult niche. Further studies will be required to determine whether it is

essential for the function of the adult niche, for example by controlling the expression of self-renewal factors.

Using RNAseq, we have generated a novel list of genes enriched in LL3/P0 ovaries, and from this list have identified several pathways potentially affected by the loss of *Lmx1a*. Within this list are several transcription factors and components of signaling pathways necessary for ovarian niche development, function and maintenance, including Hh, FGF, Notch, Engrailed and Sox100B. Indeed, RNAi-mediated knockdown of several of these transcripts within the *Lmx1a*-Gal4 lineage results in ovary developmental defects and reduced fertility. We therefore propose that *Lmx1a* controls many aspects of the development of this tissue, including proliferation, migration or cell shape changes, by regulating a series of developmental factors and signal pathways. It is important to note that our study does not allow us to distinguish between a direct transcriptional regulation of these genes by *Lmx1a* and an indirect effect of an impaired development of the TF-cap structure in *Lmx1a* mutants. Our data analyzed, in young adult females, the consequence of manipulating Hh, Sox100B, Engrailed and *Invected* in the *Lmx1a* lineage. Investigating the function of these genes, specifically during the LL3-P0 transition or later during metamorphosis or adulthood, will allow us to test whether their genetic requirement and expression are compatible with a direct regulation by *Lmx1a* and to understand better the sequence of events required for normal ovarian morphogenesis.

Interestingly, Engrailed has been previously suggested to be required for TF stacking based on clonal analysis of TF cells homozygous mutant for both Engrailed and *Invected* (Bolívar et al., 2006). Our work suggests that the stacking defects caused by these mutations lead to a mild developmental phenotype in young adults. However, consistent with other work revealing a crucial role for Engrailed in the adult niche (Eliazer et al., 2014; Luo et al., 2017; Rojas-Ríos et al., 2012), we also show that persistent knockdown of Engrailed/*Invected* well into adulthood leads to an eventual loss of ovaries. We speculate that the progressiveness of this defect is the consequence of a continuous impairment of adult niche function that worsens a mild initial developmental phenotype.

We investigated where *Lmx1a* functions in relation to the transcription factors *Bab1* and *Bab2*. In support of earlier work, we found that both *bab1* and *bab2* are required for ovary morphogenesis. In addition, we show a strong reduction in *Lmx1a* mRNA expression in the ovaries of LL3/P0 *bab1* homozygous mutant animals, placing *Bab1* genetically and/or temporally upstream of *Lmx1a*. It is worth noting that, although reduced, the expression of *Lmx1a* is not eliminated in *Bab1* mutants. We speculate that *Bab2* activity may be maintaining residual *Lmx1a* expression in this background. We found that heterozygosity for *Bab1* is sufficient to enhance the ovary developmental defects caused by RNAi-mediated knockdown of the *Lmx1a*-dependent genes tested here, consistent with our model in which the *bric-à-brac* locus lies genetically upstream of *Lmx1a*.

Finally, we found that the *Lmx1a* null homozygous phenotype can be significantly rescued by the expression of chicken *Lmx1b*, in terms of TF-cap formation, sheath formation and fertility. This reveals striking conservation between the *Lmx1a/b* factors across the animal kingdom. Even more striking is the conserved relationship between *Lmx1a/b* and Engrailed. For example, *Lmx1b* is required for Engrailed expression during both the establishment of the isthmic organizer in the developing mouse midbrain, and the specification and differentiation of dopaminergic neurons (Guo et al., 2007; Sherf et al., 2015). Additionally, simultaneous lentiviral-mediated expression of *Lmx1b* and

Engrailed has been shown to aid in the differentiation of dopaminergic neurons *in vitro* (Panman et al., 2011). Altogether, these observations point to a likely conserved *Lmx1a/b*-Engrailed transcriptional module involved in tissue patterning and cell differentiation, across different developing tissues, cell types and species. We therefore anticipate that studies on the function of *Lmx1a* in the *Drosophila* ovary will lead to a better understanding of the developmental function of *Lmx1a* in animals ranging from invertebrates to mammals. Our study also indicates that *Drosophila* represents a valuable model in which to investigate the mechanisms underlying complex diseases caused by a dysfunction of *Lmx1a/b*, such as nail-patella syndrome, ovarian carcinoma and Parkinson's disease.

## MATERIALS AND METHODS

### *Drosophila* stocks and culture

All flies were cultured on standard yeast and molasses-based food at 25°C and 65% humidity, on a 12-h light/dark cycle, unless otherwise indicated. The following stocks were obtained from the Bloomington *Drosophila* Stock Center: *Lmx1a*-Gal4 (#41248), *Gtrace* (#28280), *UAS-mCD8-GFP* (#32184), *TM3-GFP* (#4534), *Df(3L)ED4475* (#8069), *Df(3L)ED4483* (#8070), *Df(3L)BSC380* (#24404), *Lmx1a<sup>RNAi</sup> TRIP* (#31905), *bab-Gal4<sup>Agal4-5</sup>* (#6802), *bab-Gal4<sup>Pgal4-2</sup>* (#6803), *Lmx1ab-Gal4<sup>GMR35G09</sup>* (#47557), *tubGal80<sup>ts</sup>* (#7108), *Invected<sup>RNAi</sup> TRIP* (#41675), *Bab1<sup>RNAi</sup>* (#57410), *Bab2<sup>RNAi</sup>* (#49042), *TM3* (#2537), *GMR-Gal4* (#1104), *Ths-Gal4* (#47051), *Htl-Gal4* (#40669), *Chip<sup>RNAi</sup> TRIP* (#35435), *Hh<sup>RNAi</sup> TRIP* (#25794), *Sox100B<sup>RNAi</sup> TRIP* (#57417); the Vienna *Drosophila* Resource Center: *Lmx1a<sup>RNAi</sup> KK* (108747), *Lmx1a<sup>RNAi</sup> GD* (#51267), *Engrailed<sup>RNAi</sup> GD35697* (#35697), *Engrailed<sup>RNAi</sup> GD35698* (#35698), *Chip<sup>RNAi</sup> KK* (#107314), *Chip<sup>RNAi</sup> GD* (#30454); FlyORF: *UAS-Lmx1a-HA* (#F000446); Jean Louis Couderc: *bab1<sup>P</sup>* (Sahut-Barnola et al., 1995). Detailed genotypes used in this study are listed by corresponding figure in Table S2.

### Generation of *Lmx1a* knockout allele

The *Lmx1a<sup>Δ1</sup>*-dsRed fly stock was generated by a CRISPR-Cas9 homology directed repair (HDR) strategy. Sense and antisense *Lmx1a* gRNA oligos were annealed and cloned into the pBFv-U6.2B to generate a gRNA-expressing construct targeting the second exon of *Lmx1a*. 1 kb regions flanking the *Lmx1a* open reading frame were amplified using the 5' homology arm and 3' homology arm forward and reverse primer pairs and cloned on each side of the 3xP3-dsRed cassette in the pHD-DsRed-attP vector. The gRNA and HDR constructs were simultaneously injected into a nos-Cas9/CyO genetic background by Bestgene injection services. Adult F0 males were crossed individually with *TM3/TM6* virgins and F1 progeny were then screened for dsRed fluorescent eyes. *Lmx1a<sup>Δ1</sup>*-dsRed genome editing was confirmed by PCR amplification of an amplicon specific to both dsRed and the *Lmx1a* locus (outside the 3' homology arm), using the *Lmx1a<sup>Δ1</sup>*-dsRed locus detection forward and reverse primers. Initial analysis of phenotype was performed in this *TM3* balanced stock and is reported in Fig. S2B. An isogenic stock was then generated by backcrossing *Lmx1a<sup>Δ1</sup>*-dsRed virgins with *w<sup>1118</sup>* males for more than five generations and rebalanced over a GFP-marked *TM3* balancer. See Table S3 for primer sequences.

### Generation of the chicken *Lmx1b* UAS transgene

The chicken *Lmx1b* clone (pSKII-c*Lmx1b*, a gift from J. C. Izpisua Belmonte) (Vogel et al., 1995) was digested with *EcoRI* and *NotI* and the c*Lmx1b* cDNA was subcloned into the corresponding sites of the pUAST vector to generate pUAS-c*Lmx1b*. The resulting clone was verified by sequencing and injected into yw embryos by standard P-element transformation.

### Ovarian phenotype scoring

Adult ovaries were scored based on a four-category scale: strong phenotype – little to no ovariole material present in dissected adult females; mild phenotype – reduced ovariole material compared with control with

substantial disruption of ovariole architecture (ovarioles not aligned from anterior to posterior or evidence of egg chamber fusion or loss of sheath) and/or evidence of detached eggs in the abdominal cavity during dissection; weak phenotype – similar ovariole material compared with control but with some mild evidence of disruption of ovariole architecture; normal.

### Fertility assay

Four females were placed with at least six healthy males in a fresh vial containing standard food. The vial was flipped every 24 h and the number of eggs laid on top of the food was counted per day over the course of 5–11 days (Fig. 2A, 5 days; Fig. 3A, 5 days; Fig. 3C, 8 days; Fig. 7C, 6 days; Fig. S3B, 8–9 days). At least four independent crosses were analyzed per genotype. The number of eggs laid/female/day was averaged over all the replicates to generate mean $\pm$ s.e.m.

Male fertility was determined by placing single males in a vial containing four healthy virgin females. Adult progeny per female per day, rather than eggs laid, was calculated as a measure of male fertility, due to the fact that females are capable of laying unfertilized eggs.

Significance was determined by Student's *t*-tests across indicated genetic conditions.

### Temporal expression of UAS-linked transgenes

The temporal and regional gene expression targeting (TARGET) system was used to temporally restrict the activity of *Lmx1a*-Gal4. We combined a ubiquitously expressed temperature-sensitive inhibitor of Gal4 (tubGal80<sup>ts</sup>) with *Lmx1a*-Gal4, along with either UAS-*Lmx1a*-HA (FlyORF) for rescue experiments or UAS-*Lmx1a*<sup>RNAi</sup> for knockdown. Flies were cultured at the Gal80<sup>ts</sup> permissive temperature (18°C) to inhibit UAS activation, and placed at 29°C to relieve Gal4 of Gal80<sup>ts</sup> repression and allow for UAS activation. Based on our observations of developmental timing at 18°C, we designated 7 days at 18°C as representative of ML3 and 10 days at 18°C as representative of 24 h post-pupariation (P24 h). The four temperature time-course conditions used in Fig. 4 are therefore as follows: 18°C throughout development, 29°C throughout development, 7 days (up until ~ML3) at 18°C followed by 29°C, and 10 days (up until ~P24 h) at 18°C followed by 29°C.

### Staging, dissection and immunostaining

LL3 larvae were selected for by their size and 'wandering' behavior. P0 animals were selected for as strictly white pupae. Dissection of these early stages was performed in PBS. The entire contents of the LL3/P0 animal was exposed using a pair of fine forceps, and fixed at room temperature for 25 min with 100 mM glutamic acid, 25 mM KCl, 20 mM MgSO<sub>4</sub>, 4 mM sodium phosphate, 1 mM MgCl<sub>2</sub>, 5% formaldehyde. This was followed by two washes with 1% Triton X-100 in PBS, the first for 5 min and the second for 30 min. All subsequent washes and immunostaining were performed with 0.3% xPBTB (0.3% Triton X-100, 1% bovine serum albumin in PBS). After completion of staining, pieces of fat body containing ovary were mounted in Mowiol-DABCO. All images of LL3 and P0 staged ovaries were taken with a Leica Sp6 confocal microscope. For each image, a single representative *z*-section was chosen from a collection of *z*-sections spanning the entire developing ovary. This chosen *z*-section was consistently selected to reveal both maximal TF architecture as well as the maximum diameter of the ovary, regardless of genotype.

Mature adult ovaries used in this study were from females that were allowed to mate over the course of 2–3 days post-eclosion. The virgin female flies presented in Fig. S2A were selected for as freshly emerged, bloated females lacking pigmentation. Eleven-day-old flies were dissected for some of the experiments reported in Fig. 7. Adult ovaries were dissected under PBS and fixed at room temperature for 45 min with 100 mM glutamic acid, 25 mM KCl, 20 mM MgSO<sub>4</sub>, 4 mM sodium phosphate, 1 mM MgCl<sub>2</sub>, 4% formaldehyde. All subsequent wash steps and immunostaining were performed with 0.5% bovine serum albumin, 0.1% Triton X-100 in PBS. Ovary pairs were mounted in Mowiol-DABCO. All images of adult ovaries in this study were taken with a Zeiss AxioImager epifluorescence microscope, except for images of ovaries from newly eclosed females in Fig. S2B, which were obtained using a Leica Sp6 confocal microscope.

The primary antibodies used in this study were all from the Developmental Studies Hybridoma Bank: mouse anti-Engrailed/Invected (4D9; 1:20), rat anti-DE-Cadherin (DCAD2; 1:20), mouse anti-Fasciclin II (1D4; 1:10), mouse anti-Fasciclin III (7G10; 1:5), mouse anti- $\alpha$ -Spectrin (3A9; 1:100), mouse anti- $\beta$ -galactosidase (40-1a; 1:20). The following secondary antibodies were used in this study: Cy5-conjugated goat anti-mouse, Cy5-conjugated goat anti-rat, Alexa Fluor 488-conjugated goat anti-rat (all from Jackson ImmunoResearch; 1:500). Alexa Fluor 633-Phalloidin was used at a concentration of 1:400 to stain for muscular sheath. Hoechst 33342 was used at a concentration of 1:2000 to stain DNA.

All confocal images presented are single *z*-sections. Images imported in Adobe Photoshop and figures assembled using Adobe Illustrator.

### Analysis of gene expression by real-time qPCR

Fat body samples with or without ovary were dissected in PBS as described above. Twenty-four pairs per sample were placed into 300  $\mu$ l total of RLT buffer (provided by RNeasy Qiagen kit) and frozen immediately at –80°C. Once all samples were prepared, they were thawed, vortexed briefly and RNAs isolated using the RNeasy Qiagen kit. Superscript II enzyme was used to reverse transcribe 680 ng of total RNA per sample. Real-time PCR was performed on a Biorad MyiQ. The primers used to amplify *Actin 5C*, *vasa*, *bab1*, *bab2*, *Fbp2*, *Hh*, *Ser* and *Lmx1a* are detailed in Table S3.

### RNA sequencing

RNA (500 ng) was extracted from dissected fat bodies with or without ovaries and submitted for RNA sequencing at the University of Rochester Genomic Research Center. Raw reads generated from the Illumina HiSeq2500 sequencer were demultiplexed using `configurebcl2fastq.pl` version 1.8.4. Quality filtering and adapter removal are performed using Trimmomatic version 0.36 with the following parameters: 'SLIDINGWINDOW:4:20 TRAILING:13 LEADING:13 ILLUMINACLIP:adapters.fasta:2:30:10 MINLEN:15'. Processed/cleaned reads were then mapped to the *D. melanogaster* reference genome (dm6) with STAR\_2.5.2b with the following parameters: '-twopassMode Basic -runMode alignReads -outSAMtype BAM SortedByCoordinate -outSAMstrandField intronMotif -outFilterIntronMotifs RemoveNoncanonical -outReadsUnmapped Fastx'. Gene-level read quantification was derived using feature counts from the subread-1.5.0p3 package with the dm6 GTF annotation file and the following parameters: '-s 0 -t exon -g gene\_name'. Differential expression analysis was performed using DESeq2-1.14.1 with an adjusted *P*-value threshold of 0.05 within R version 3.3.2. Heat maps were generated using ggplot2 after normalizing all values to the median value of *Lmx1a*<sup>Δ1/+</sup> FatBody+Ovaries samples for each gene. The volcano plot was generated using the same package.

### Acknowledgements

We are grateful to Dirk Bohmann for comments on the manuscript and Dan Bergstrahl and members of the Bateau lab for helpful discussions. We would like to thank Victor Zhang for his technical assistance with this project; Jean-Louis Couderc, the Bloomington *Drosophila* Stock Center, the Vienna *Drosophila* Resource Center and the Zurich ORFeome Project for fly lines; and the Developmental Studies Hybridoma Bank, created by the NICHD of the NIH and maintained at The University of Iowa, for antibodies. RNAseq library construction, sequencing, and primary analysis were performed by the Genomics Research Center at the University of Rochester.

### Competing interests

The authors declare no competing or financial interests.

### Author contributions

Conceptualization: A.W.A., B.B.; Methodology: A.W.A., B.B.; Formal analysis: A.W.A.; Investigation: A.W.A.; Resources: D.E.R.-L.; Writing - original draft: A.W.A., B.B.; Writing - review & editing: A.W.A., D.E.R.-L., B.B.; Supervision: B.B.; Project administration: B.B.; Funding acquisition: B.B.

### Funding

This work was supported by grants from the National Institutes of Health to B.B. (R01GM108712) and a Medical Scientist Training Program training grant from the National Institutes of Health (T32GM735637) to A.W.A. Deposited in PMC for release after 12 months.

## Data availability

Raw and analyzed RNA sequencing data have been deposited to the Gene Expression Omnibus under accession number GSE109258.

## Supplementary information

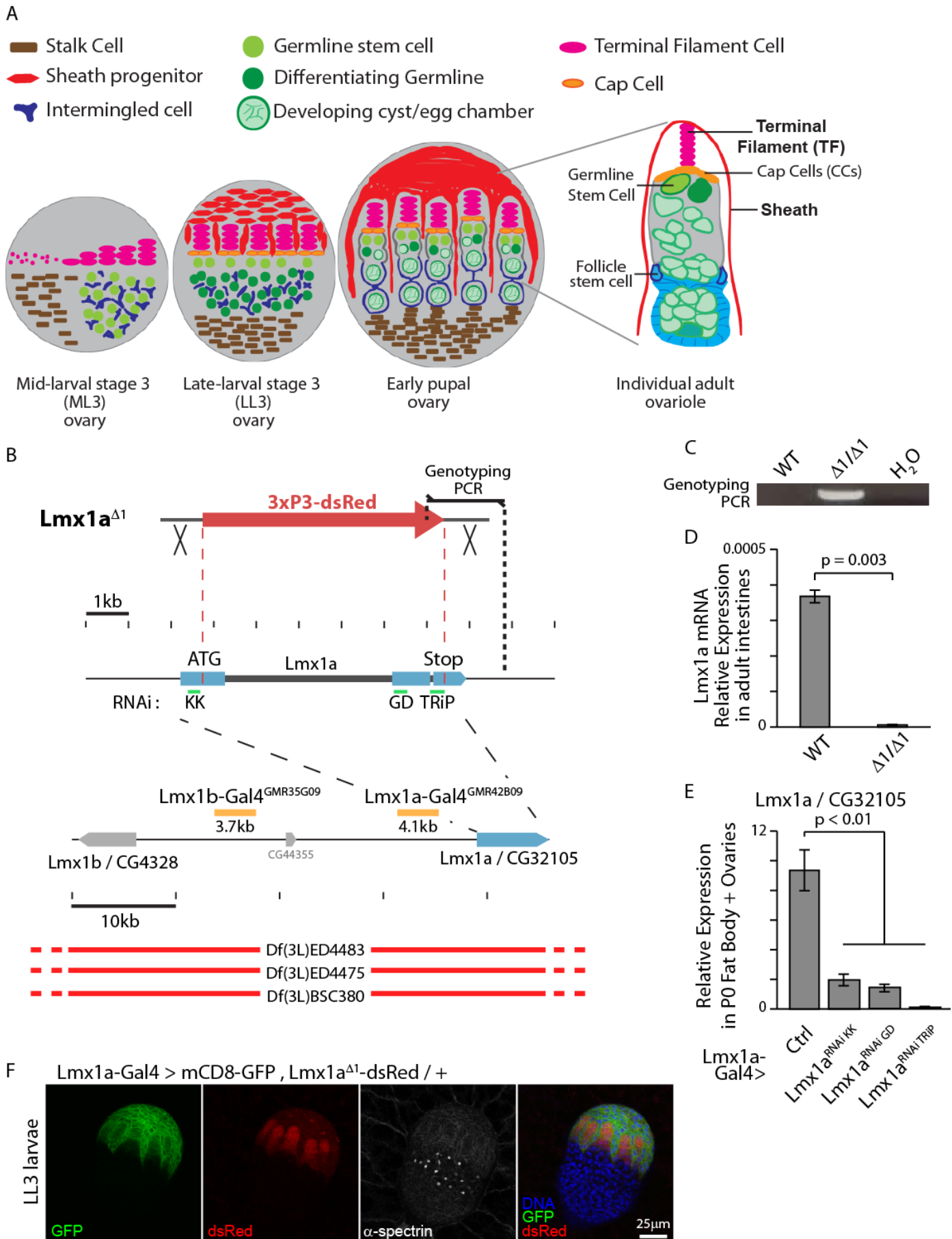
Supplementary information available online at <http://dev.biologists.org/lookup/doi/10.1242/dev.163394.supplemental>

## References

- Andersson, E., Tryggvason, U., Deng, Q., Friling, S., Alekseenko, Z., Robert, B., Perlmann, T. and Ericson, J. (2006). Identification of intrinsic determinants of midbrain dopamine neurons. *Cell* **124**, 393-405.
- Bartoletti, M., Rubin, T., Chalvet, F., Netter, S., Dos Santos, N., Poisot, E., Paces-Fessy, M., Cumenal, D., Peronnet, F., Pret, A. M. et al. (2012). Genetic basis for developmental homeostasis of germline stem cell niche number: a network of Tramtrack-Group nuclear BTB factors. *PLoS ONE* **7**, e49958.
- Bolívar, J., Pearson, J., Lopez-Onieva, L. and Gonzalez-Reyes, A. (2006). Genetic dissection of a stem cell niche: the case of the Drosophila ovary. *Dev. Dyn.* **235**, 2969-2979.
- Bongers, E. M., de Wijs, I. J., Marcellis, C., Hoefsloot, L. H. and Knoers, N. V. (2008). Identification of entire LMX1B gene deletions in nail patella syndrome: evidence for haploinsufficiency as the main pathogenic mechanism underlying dominant inheritance in man. *Eur. J. Hum. Genet.* **16**, 1240-1244.
- Boyle, M. and DiNardo, S. (1995). Specification, migration and assembly of the somatic cells of the Drosophila gonad. *Development* **121**, 1815-1825.
- Burghardt, T., Kastner, J., Suleiman, H., Rivera-Milla, E., Stepanova, N., Lottaz, C., Kubitz, M., Boger, C. A., Schmidt, S., Gorski, M. et al. (2013). LMX1B is essential for the maintenance of differentiated podocytes in adult kidneys. *J. Am. Soc. Nephrol.* **24**, 1830-1848.
- Cabrera, G. R., Godt, D., Fang, P.-Y., Couderc, J.-L. and Laski, F. A. (2002). Expression pattern of Gal4 enhancer trap insertions into the bric a brac locus generated by P element replacement. *Genesis* **34**, 62-65.
- Chen, H., Lun, Y., Ovchinnikov, D., Kokubo, H., Oberg, K. C., Pepicelli, C. V., Gan, L., Lee, B. and Johnson, R. L. (1998). Limb and kidney defects in Lmx1b mutant mice suggest an involvement of LMX1B in human nail patella syndrome. *Nat. Genet.* **19**, 51-55.
- Couderc, J. L., Godt, D., Zollman, S., Chen, J., Li, M., Tiong, S., Cramton, S. E., Sahut-Barnola, I. and Laski, F. A. (2002). The bric a brac locus consists of two paralogous genes encoding BTB/POZ domain proteins and acts as a homeotic and morphogenetic regulator of imaginal development in Drosophila. *Development* **129**, 2419-2433.
- Ding, Y.-Q., Marklund, U., Yuan, W., Yin, J., Wegman, L., Ericson, J., Deneris, E., Johnson, R. L. and Chen, Z. F. (2003). Lmx1b is essential for the development of serotonergic neurons. *Nat. Neurosci.* **6**, 933-938.
- Doucet-Beaupré, H., Ang, S.-L. and Lévesque, M. (2015). Cell fate determination, neuronal maintenance and disease state: The emerging role of transcription factors Lmx1a and Lmx1b. *FEBS Lett.* **589**, 3727-3738.
- Dreyer, S. D., Zhou, G., Baldini, A., Winterpacht, A., Zabel, B., Cole, W., Johnson, R. L. and Lee, B. (1998). Mutations in LMX1B cause abnormal skeletal patterning and renal dysplasia in nail patella syndrome. *Nat. Genet.* **19**, 47-50.
- Edwards, N., Rice, S. J., Raman, S., Hynes, A. M., Srivastava, S., Moore, I., Al-Hamed, M., Xu, Y., Santibanez-Koref, M., Thwaites, D. T. et al. (2015). A novel LMX1B mutation in a family with end-stage renal disease of 'unknown cause'. *Clin. Kidney J.* **8**, 113-119.
- Eliazer, S. and Buszczak, M. (2011). Finding a niche: studies from the Drosophila ovary. *Stem Cell Res.* **2**, 45.
- Eliazer, S., Palacios, V., Wang, Z., Kollipara, R. K., Kittler, R. and Buszczak, M. (2014). Lsd1 restricts the number of germline stem cells by regulating multiple targets in escort cells. *PLoS Genet.* **10**, e1004200.
- Evans, C. J., Olson, J. M., Ngo, K. T., Kim, E., Lee, N. E., Kuoy, E., Patananan, A. N., Sitz, D., Tran, P., Do, M. T. et al. (2009). G-TRACE: rapid Gal4-based cell lineage analysis in Drosophila. *Nat. Methods* **6**, 603-605.
- Forbes, A. J., Lin, H., Ingham, P. W. and Spradling, A. C. (1996). hedgehog is required for the proliferation and specification of ovarian somatic cells prior to egg chamber formation in Drosophila. *Development* **122**, 1125-1135.
- Gancz, D. and Gilboa, L. (2013). Insulin and Target of rapamycin signaling orchestrate the development of ovarian niche-stem cell units in Drosophila. *Development* **140**, 4145-4154.
- Gancz, D., Lengil, T. and Gilboa, L. (2011). Coordinated regulation of niche and stem cell precursors by hormonal signaling. *PLoS Biol.* **9**, e1001202.
- German, M. S., Wang, J., Chadwick, R. B. and Rutter, W. J. (1992). Synergistic activation of the insulin gene by a LIM-homeo domain protein and a basic helix-loop-helix protein: building a functional insulin minienhancer complex. *Genes Dev.* **6**, 2165-2176.
- Gilboa, L. (2015). Organizing stem cell units in the Drosophila ovary. *Curr. Opin. Genet. Dev.* **32**, 31-36.
- Godt, D. and Laski, F. A. (1995). Mechanisms of cell rearrangement and cell recruitment in Drosophila ovary morphogenesis and the requirement of bric a brac. *Development* **121**, 173-187.
- Green, D. A. and Extavour, C. G. II (2014). Insulin signalling underlies both plasticity and divergence of a reproductive trait in Drosophila. *Proc. Biol. Sci.* **281**, 20132673.
- Guo, C., Qiu, H.-Y., Huang, Y., Chen, H., Yang, R.-Q., Chen, S.-D., Johnson, R. L., Chen, Z.-F. and Ding, Y.-Q. (2007). Lmx1b is essential for Fgf8 and Wnt1 expression in the isthmus organizer during tectum and cerebellum development in mice. *Development* **134**, 317-325.
- He, L., Guo, L., Vathipadiekal, V., Sergeant, P. A., Growdon, W. B., Engler, D. A., Rueda, B. R., Birrer, M. J., Orsulic, S. and Mohapatra, G. (2014). Identification of LMX1B as a novel oncogene in human ovarian cancer. *Oncogene* **33**, 4226-4235.
- Hobert, O. and Westphal, H. (2000). Functions of LIM-homeobox genes. *Trends Genet.* **16**, 75-83.
- Hodin, J. and Riddiford, L. M. (1998). The ecdysone receptor and ultraspiracle regulate the timing and progression of ovarian morphogenesis during Drosophila metamorphosis. *Dev. Genes Evol.* **208**, 304-317.
- Irizarry, J. and Stathopoulos, A. (2015). FGF signaling supports Drosophila fertility by regulating development of ovarian muscle tissues. *Dev. Biol.* **404**, 1-13.
- Kirilly, D. and Xie, T. (2007). The Drosophila ovary: an active stem cell community. *Cell Res.* **17**, 15-25.
- Laguna, A., Schintu, N., Nobre, A., Alvarsson, A., Volakakis, N., Jacobsen, J. K., Gomez-Galan, M., Sopova, E., Joodmardi, E., Yoshitake, T. et al. (2015). Dopaminergic control of autophagic-lysosomal function implicates Lmx1b in Parkinson's disease. *Nat. Neurosci.* **18**, 826-835.
- Lengil, T., Gancz, D. and Gilboa, L. (2015). Activin signaling balances proliferation and differentiation of ovarian niche precursors and enables adjustment of niche numbers. *Development* **142**, 883-892.
- Lin, C. K., Chao, T. K., Lai, H. C. and Lee, H. S. (2012). LMX1A as a prognostic marker in ovarian mucinous cystadenocarcinoma. *Am. J. Clin. Pathol.* **137**, 971-977.
- Luo, L., Siah, C. K. and Cai, Y. (2017). Engrailed acts with Nejire to control decapentaplegic expression in the Drosophila ovarian stem cell niche. *Development* **144**, 3224-3231.
- McIntosh, I., Dreyer, S. D., Clough, M. V., Dunston, J. A., Eyaid, W., Roig, C. M., Montgomery, T., Ala-Mello, S., Kaitila, I., Winterpacht, A. et al. (1998). Mutation analysis of LMX1B gene in nail-patella syndrome patients. *Am. J. Hum. Genet.* **63**, 1651-1658.
- Miner, J. H., Morello, R., Andrews, K. L., Li, C., Antignac, C., Shaw, A. S. and Lee, B. (2002). Transcriptional induction of slit diaphragm genes by Lmx1b is required in podocyte differentiation. *J. Clin. Invest.* **109**, 1065-1072.
- Morello, R., Zhou, G., Dreyer, S. D., Harvey, S. J., Ninomiya, Y., Thorne, P. S., Miner, J. H., Cole, W., Winterpacht, A., Zabel, B. et al. (2001). Regulation of glomerular basement membrane collagen expression by LMX1B contributes to renal disease in nail patella syndrome. *Nat. Genet.* **27**, 205-208.
- Nanda, S., DeFalco, T. J., Loh, S. H., Phochanukul, N., Camara, N., Van Doren, M. and Russell, S. (2009). Sox100B, a Drosophila group E Sox-domain gene, is required for somatic testis differentiation. *Sex. Dev.* **3**, 26-37.
- Panman, L., Andersson, E., Alekseenko, Z., Hedlund, E., Kee, N., Mong, J., Uhde, C. W., Deng, Q., Sandberg, R., Stanton, L. W. et al. (2011). Transcription factor-induced lineage selection of stem-cell-derived neural progenitor cells. *Cell Stem Cell* **8**, 663-675.
- Pressman, C. L., Chen, H. and Johnson, R. L. (2000). LMX1B, a LIM homeodomain class transcription factor, is necessary for normal development of multiple tissues in the anterior segment of the murine eye. *Genesis* **26**, 15-25.
- Rohr, C., Prestel, J., Heidet, L., Hosser, H., Kriz, W., Johnson, R. L., Antignac, C. and Witzgall, R. (2002). The LIM-homeodomain transcription factor Lmx1b plays a crucial role in podocytes. *J. Clin. Invest.* **109**, 1073-1082.
- Roignant, J. Y., Legent, K., Janody, F. and Treisman, J. E. (2010). The transcriptional co-factor Chip acts with LIM-homeodomain proteins to set the boundary of the eye field in Drosophila. *Development* **137**, 273-281.
- Rojas-Ríos, P., Guerrero, I. and González-Reyes, A. (2012). Cytoneme-mediated delivery of hedgehog regulates the expression of bone morphogenetic proteins to maintain germline stem cells in Drosophila. *PLoS Biol.* **10**, e1001298.
- Sahut-Barnola, I., Godt, D., Laski, F. A. and Couderc, J.-L. (1995). Drosophila ovary morphogenesis: analysis of terminal filament formation and identification of a gene required for this process. *Dev. Biol.* **170**, 127-135.
- Sarikaya, D. P. and Extavour, C. G. (2015). The Hippo pathway regulates homeostatic growth of stem cell niche precursors in the Drosophila ovary. *PLoS Genet.* **11**, e1004962.
- Sherf, O., Nashelsky Zolotov, L., Liser, K., Tilleman, H., Jovanovic, V. M., Zega, K., Jukic, M. M. and Brodski, C. (2015). Otx2 requires Lmx1b to control the development of mesodiencephalic dopaminergic neurons. *PLoS ONE* **10**, e0139697.
- Song, X., Call, G. B., Kirilly, D. and Xie, T. (2007). Notch signaling controls germline stem cell niche formation in the Drosophila ovary. *Development* **134**, 1071-1080.
- Tsai, W.-C., Lee, H.-S., Lin, C.-K., Chen, A., Nieh, S. and Ma, H.-I. (2012). The association of osteopontin and LMX1A expression with World Health Organization grade in meningiomas and gliomas. *Histopathology* **61**, 844-856.

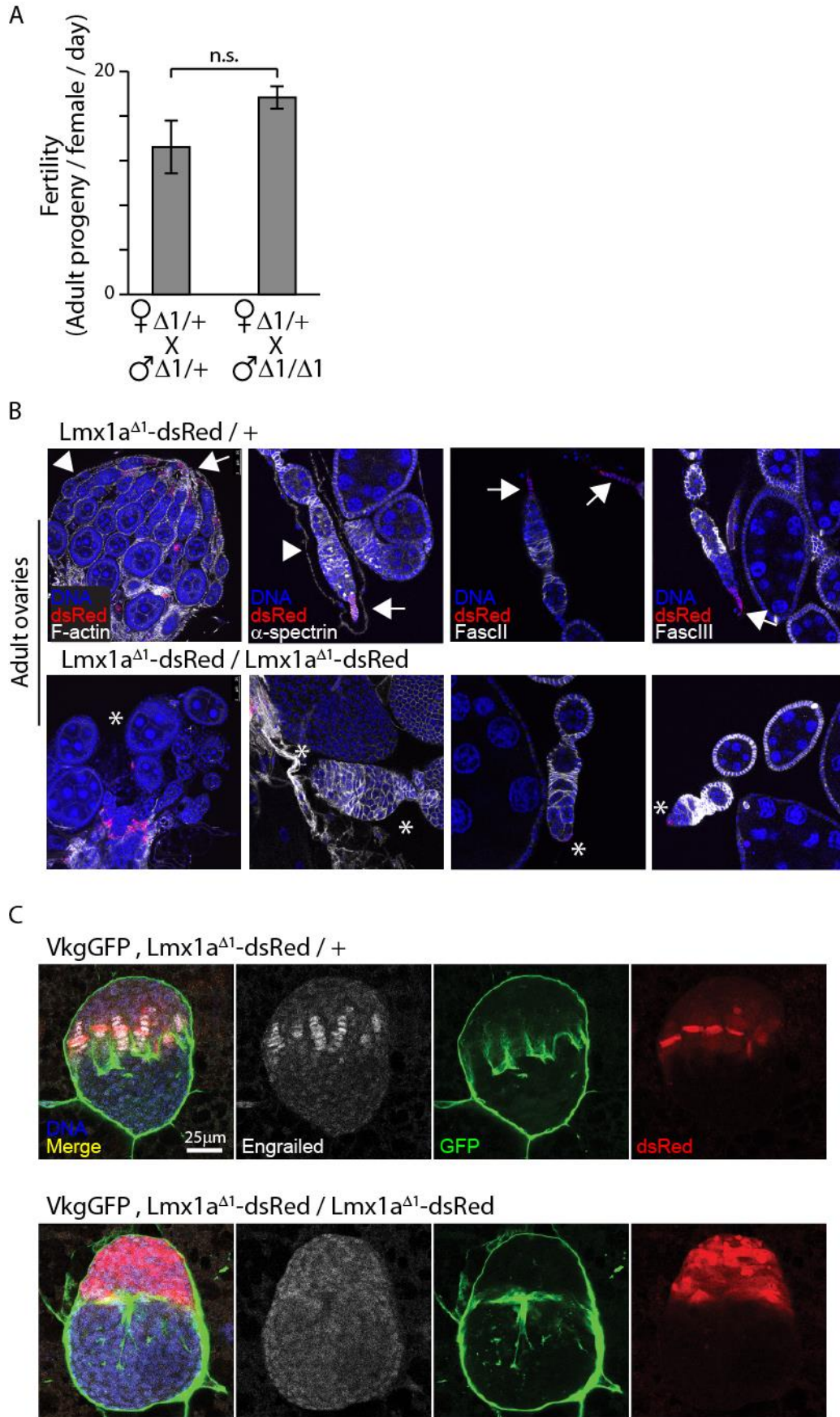
- Tsai, W.-C., Lin, C.-K., Yang, Y.-S., Chan, D.-C., Gao, H.-W., Chang, F.-N. and Jin, J.-S.** (2013). The correlations of LMX1A and osteopontin expression to the clinicopathologic stages in pancreatic adenocarcinoma. *Appl. Immunohistochem. Mol. Morphol.* **21**, 395-400.
- Van De Bor, V., Zimniak, G., Papone, L., Cerezo, D., Malbouyres, M., Juan, T., Ruggiero, F. and Noselli, S.** (2015). Companion blood cells control ovarian stem cell niche microenvironment and homeostasis. *Cell Rep.* **13**, 546-560.
- Vogel, A., Rodriguez, C., Warnken, W. and Izpisua Belmonte, J. C.** (1995). Dorsal cell fate specified by chick Lmx1 during vertebrate limb development. *Nature* **378**, 716-720.
- Vollrath, D., Jaramillo-Babb, V. L., Clough, M. V., McIntosh, I., Scott, K. M., Lichter, P. R. and Richards, J. E.** (1998). Loss-of-function mutations in the LIM-homeodomain gene, LMX1B, in nail-patella syndrome. *Hum. Mol. Genet.* **7**, 1091-1098.
- Wang, P., Chen, Y., Li, C., Zhao, R., Wang, F., Lin, X., Cao, L., Li, S., Hu, L., Gao, Y. et al.** (2016). Drosophila eye developmental defect caused by elevation of the activity of the LIM-homeodomain protein, Lmx1a, requires its association with the Co-activator Chip. *Biochem. Biophys. Res. Commun.* **470**, 29-34.
- Xie, T. and Spradling, A. C.** (1998). decapentaplegic is essential for the maintenance and division of germline stem cells in the Drosophila ovary. *Cell* **94**, 251-260.

**Supplementary Information (7 figures and 3 tables)**

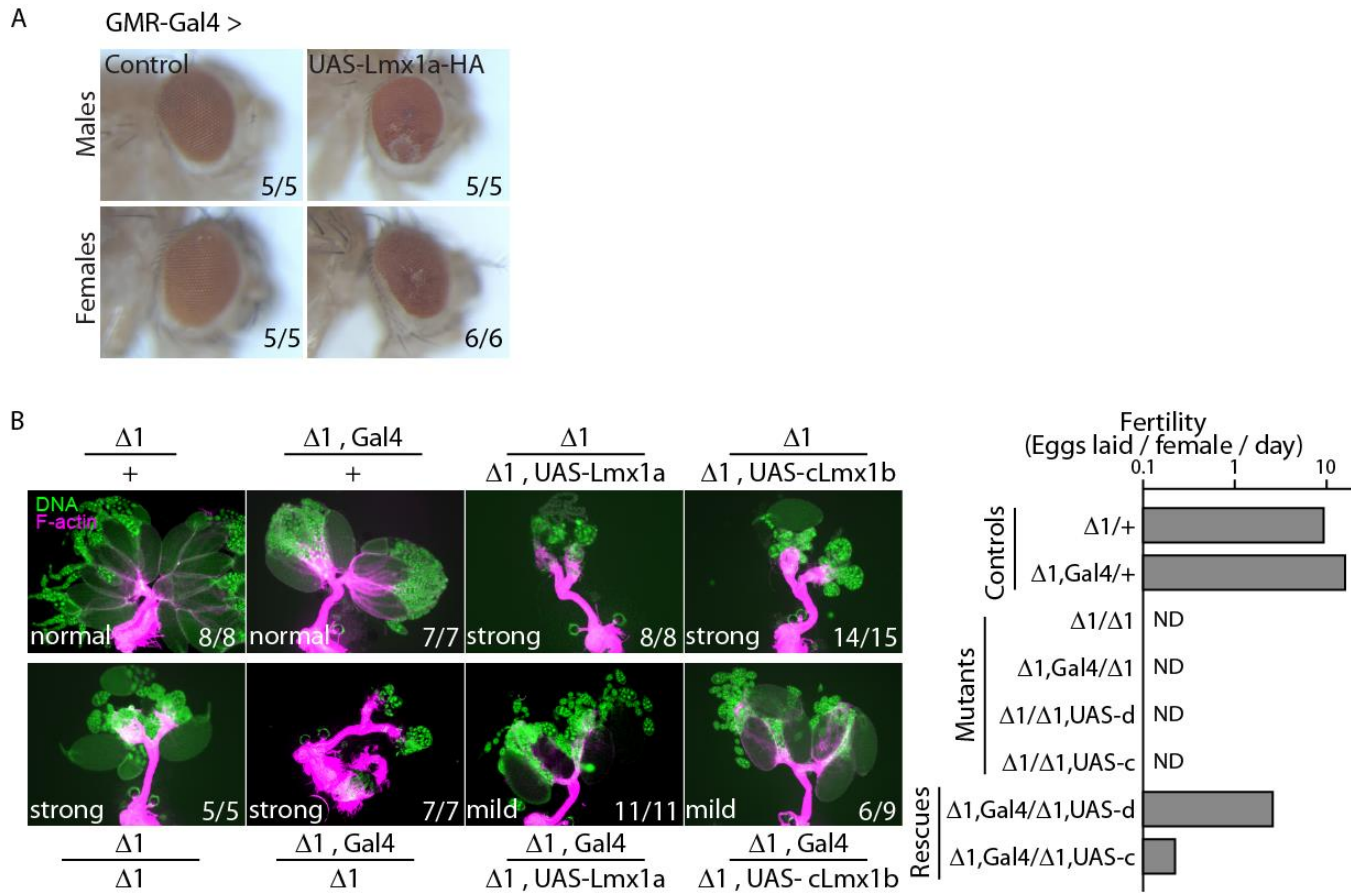


**Supplementary Figure 1. Drosophila ovary development, the Lmx1a locus, Lmx1a knock out allele and confirmed Lmx1a knock-down efficiency.** (A) Schematic representation of Drosophila ovary development and the main cell types involved, from larval stages to adulthood. The terminal filament and cap cells form the stem cell niche in each ovariole. (B) Schematic of the Lmx1a locus and tools used to manipulate its expression. Shown at top is the strategy to generate Lmx1a<sup>Δ1</sup>-dsRed via Cas9-mediated double strand break and Homology Directed Repair (HDR), replacing the Lmx1a open reading frame with 3xP3-dsRed. The designed gRNA sequence directed Cas9 to the second exon. The 1kb homology arms of the HDR construct are indicated. Indicated in green are the regions targeted by the three RNAi constructs used to knock-down Lmx1a expression in this study. Below is indicated where the Lmx1a locus lies in relation to Lmx1b/CG4328 as well as the locations of the enhancer regions represented by the Lmx1a-Gal4 and Lmx1b/a-Gal4 lines used. The three red lines below indicate that the three deficiency lines used to validate the Lmx1a<sup>Δ1</sup>-dsRed phenotype span the full locus of Lmx1a and dLmx1b. (C) Validation of the Lmx1a<sup>Δ1</sup>-dsRed insertion using PCR amplification of a 3' region of dsRed and the locus downstream of the 3' homology arm, as represented in (B). (D) Further validation of Lmx1a<sup>Δ1</sup>-dsRed by qPCR, showing full loss of detectable Lmx1a transcript in adult midgut mRNAs. Lmx1a expression is normalized to Actin5c. (E) Lmx1a transcript knock down efficiency of Lmx1a-Gal4-driven Lmx1a dsRNA expression as detected by qPCR relative to Vasa transcript in LL3/P0 fat bodies containing ovaries. (F) dsRed (from the Lmx1a<sup>Δ1</sup> locus) and Lmx1a-Gal4-driven GFP co-localize in terminal filaments, cap cells and apical cells within the anterior domain of the LL3 ovary, adjacent to germline marked by brightly α-spectrin positive fusomes. α-spectrin also stains plasma membranes.







**Supplementary Figure 2.  $Lmx1a^{\Delta 1}$  male fertility,  $Lmx1a^{\Delta 1}$  ovarian defects in rare genetic backgrounds where residual adult ovariole material is present, and loss of niche architecture as revealed by GFP-labeled collagen IV.** (A) Fertility assay showing that  $Lmx1a^{\Delta 1}$ -dsRed homozygous males have no defects in fertility compared to heterozygous siblings. Five cohorts of four females were analyzed per genotype. Values are presented as mean  $\pm$  s.e.m., P value is calculated using two-tailed t-test. (B) In rare genetic backgrounds, including a non-backcross  $Lmx1a^{\Delta 1}$ -dsRed/TM3 balanced stock shown here, residual ovarian tissue can be recovered from newly eclosed virgin homozygous mutant females. Left panel shows phalloidin staining and dsRed expression, revealing loss of both terminal filaments (arrows) and sheath (arrowheads) in  $Lmx1a^{\Delta 1}$ -dsRed homozygotes compared to heterozygotes. Anterior is top right, posterior is bottom left. The asterisk marks absence of sheath in mutant ovaries. The three panels to the right show zoomed-in images of mature ovaries of the same stock, again revealing the presence of terminal filaments (arrows) and sheath (arrowheads) in heterozygotes and the loss of these structures in rare ovarioles found in homozygotes (asterisks). (C) GFP-labeled collagen IV subunit (Vkg-GFP) demarcates forming TF-cap structures in control ovaries. This pattern is lost in  $Lmx1a^{\Delta 1}$  homozygotes. Loss of En/Inv immunostaining and dsRed pattern also reveal defective terminal filament development as also shown in Fig. 2 E.

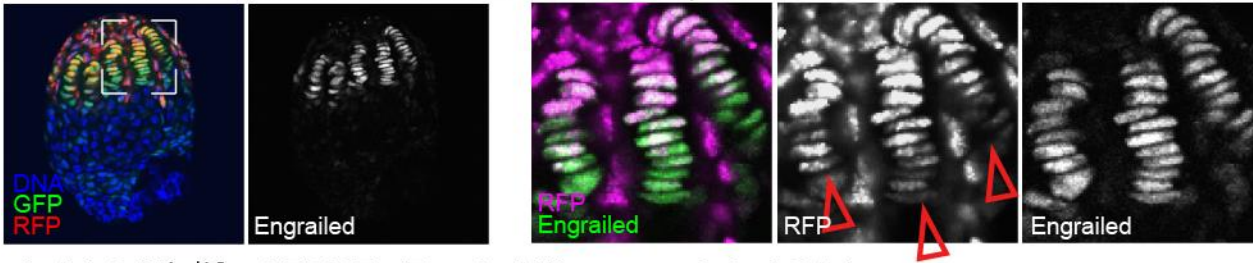


**Supplementary Figure 3. Genetic rescue by re-expression of Lmx1a and cLmx1b in developing TF-cap structures.** (A) Wang et al. reported in 2015 that ectopic expression of Lmx1a in the eye imaginal disc induces eye defects. We show that expression of the HA-tagged Lmx1a construct that we used to rescue Lmx1a function in developing TFs also causes eye-defects when expressed using the GMR-Gal4 driver. This further confirms the Lmx1a fusion protein is functional. (B) Expression of UAS-Lmx1a and UAS-cLmx1b using the Lmx1a-Gal4 driver rescues the Lmx1a <sup>$\Delta 1$</sup>  homozygous phenotype when cultured at 25°C, as shown by both ovary morphology and fertility. Rescue of Lmx1a <sup>$\Delta 1$</sup> -dsRed homozygous fertility by cLmx1b appears less pronounced at 25°C, as compared to 18°C shown in figure 3A. For each condition, the severity of the phenotype and the proportion of ovary pairs observed are indicated. ND, No laid eggs Detected. Three to four cohorts of four females were analyzed per genotype. Values are presented as mean +/- s.e.m. and P values are calculated using two-tailed t-test.

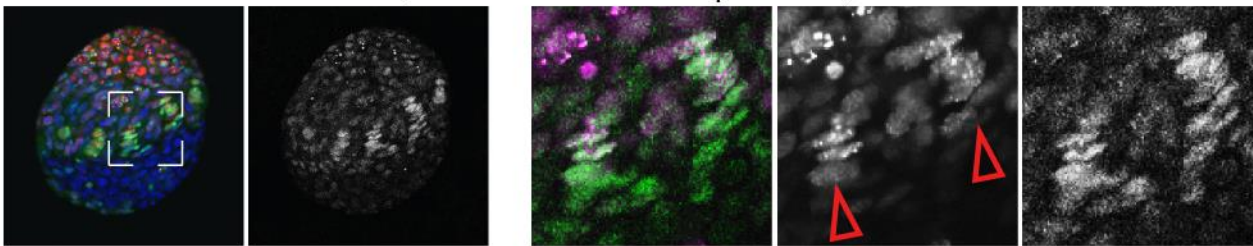
RFP expression = Driver activity in LL3 / P0 stages  
 GFP expression = Lineage tracing

	Terminal Filament in which the driver is active during the LL3/P0 transition		Terminal Filament without driver activity during the LL3/ P0 transition
---	--	---	---

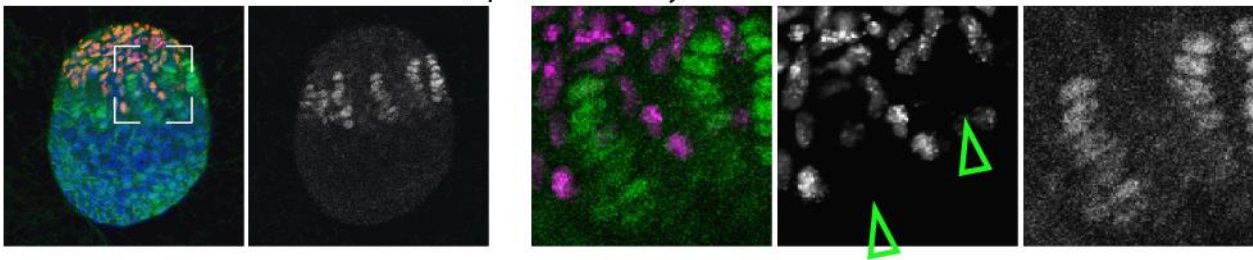
Lmx1a-Gal4 > G-TRACE (Terminal Filaments + Apical Cells)



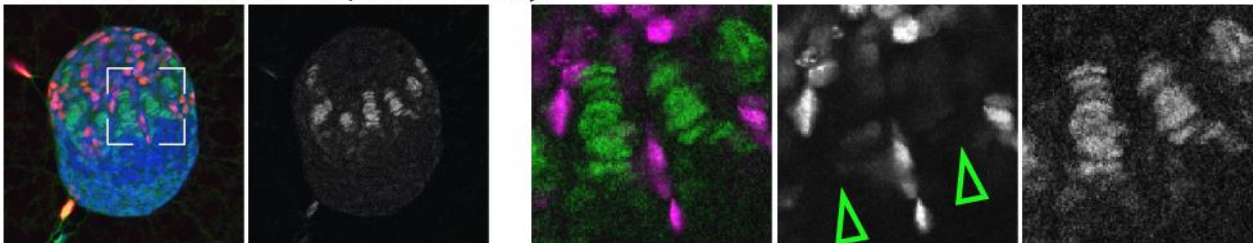
bab1-Gal4<sup>Agal4-5</sup> > G-TRACE (Terminal Filaments + Apical Cells)



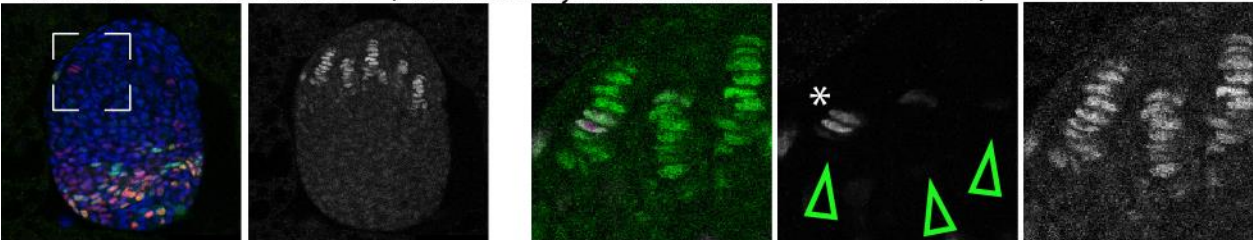
Lmx1b-Gal4<sup>GMR35G09</sup> > G-TRACE (Apical Cells only)



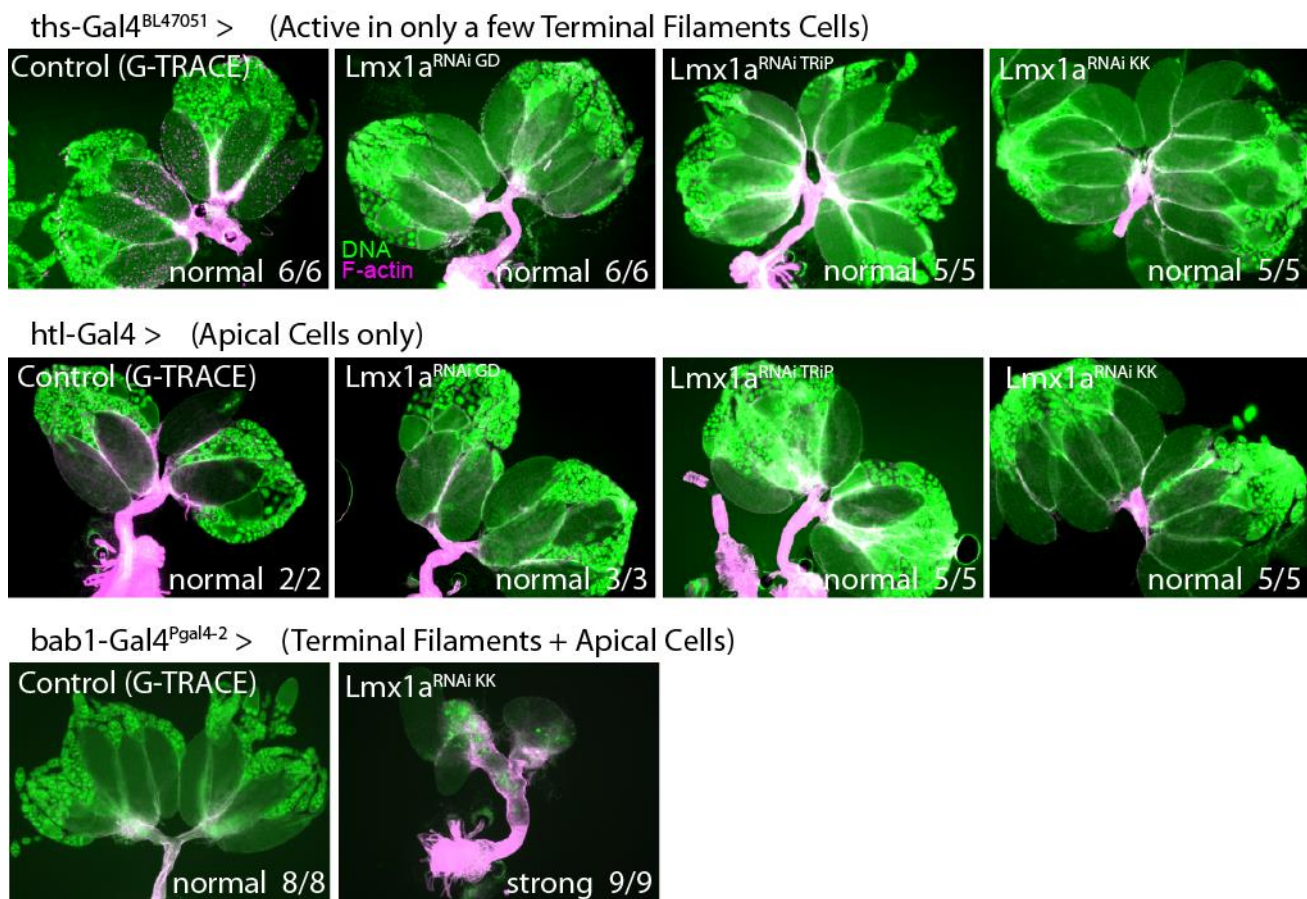
Htl-Gal4 > G-TRACE (Apical Cells only)



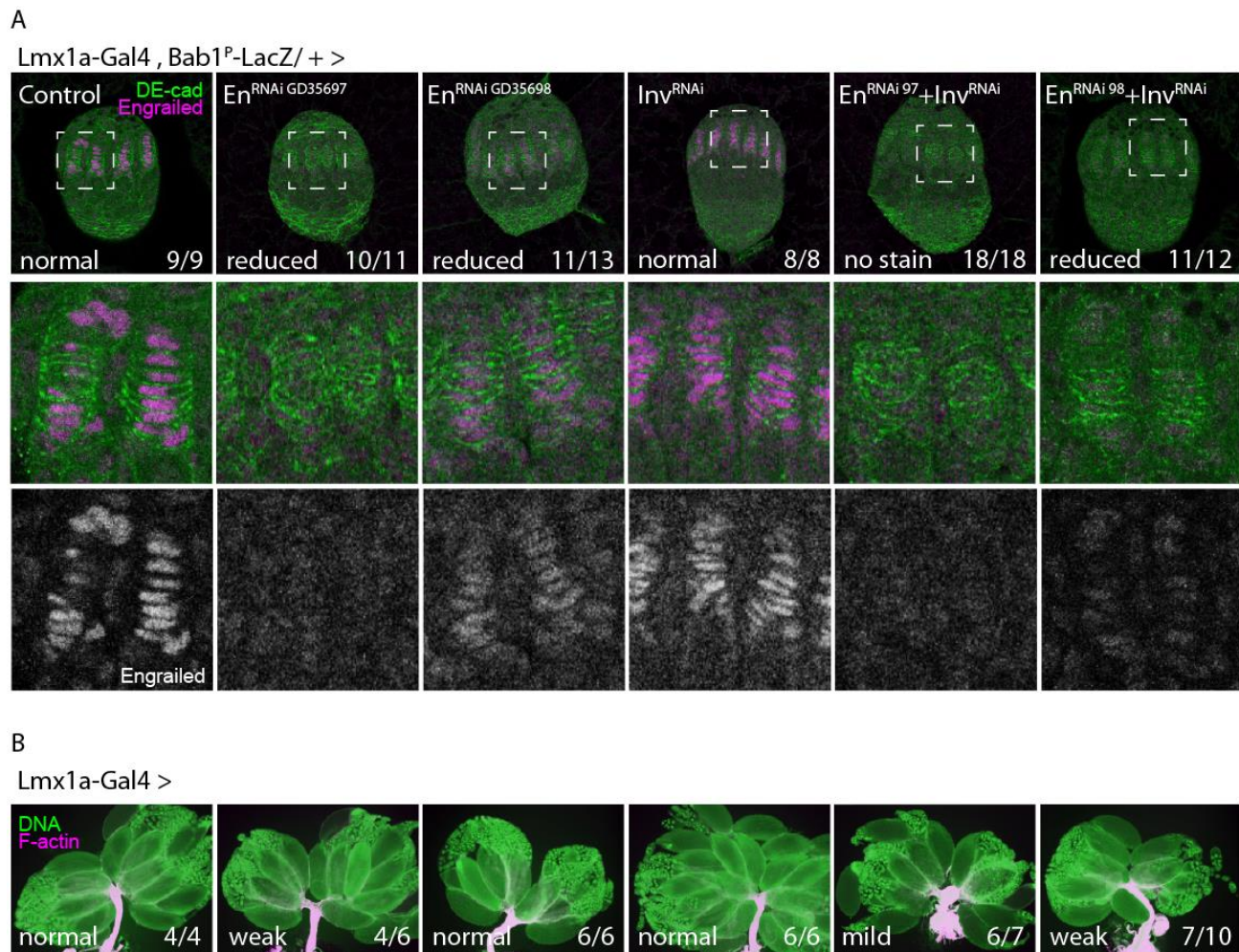
ths-Gal4<sup>BL47051</sup> > G-TRACE (Active in only a few Terminal Filaments Cells)



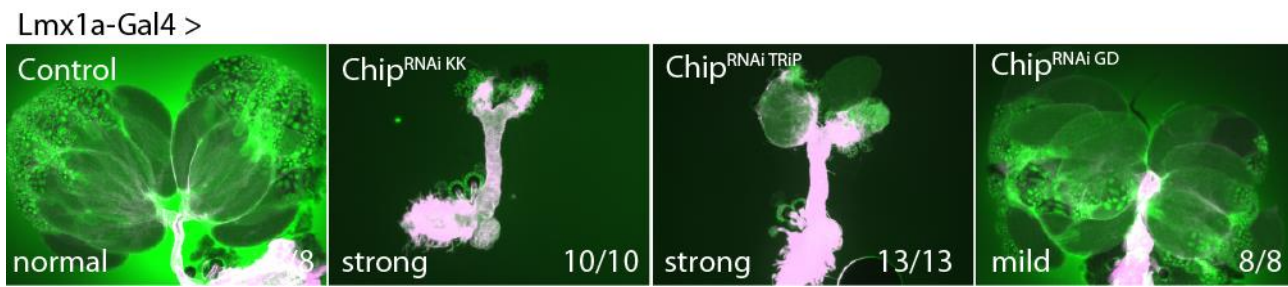
**Supplementary Figure 4. P0 expression patterns of Gal4 lines used to demonstrate the requirement of Lmx1a specifically in forming TF-cap structures.** All Gal4 driver lines were crossed with the G-TRCAE reporter to both permanently label each driver's full lineage (GFP) and mark current Gal4 activity (RFP) at the time of fixation (P0). Lmx1a-Gal4 and bab1-Gal4<sup>Agal4-5</sup> demonstrate activity in both TFs and apical cells at P0 (red arrowheads). dLmx1b-Gal4<sup>GMR35G09</sup>, which represents control of Gal4 by an enhancer region upstream of the dLmx1b locus, demonstrates activity in only apical cells at P0, not in TFs (green arrowheads). Htl-Gal4, as previously reported by Irizarry et al. 2015, also demonstrates activity in only apical cells at P0. Also reported by Irizarry et al. 2015, a Gal4 driver under the influence of the thisbe (ths) locus, which encodes an FGF ligand secreted by terminal filaments, drives expression specifically in terminal filaments. However, GTRACE RFP analysis of this Gal4 line reveals expression only in a small subset of TF-cap cells (asterisk) by the time of larval-pupal transition. This suggests that this driver expresses Gal4 in TF-cap structures after the time at which they form.



**Supplementary Figure 5. Additional tissue-specific Lmx1a knock-down further demonstrates the specificity of Lmx1a requirement to TF-cap structures.** ths-Gal4<sup>BL47051</sup>, which drives expression in only a small subset of terminal filament cells by the time of larval-pupal transition, does not induce adult ovary defects based on ovariole (Hoechst) and sheath (F-actin) morphology. htl-Gal4, an additional Gal4 line active only in apical cells at P0, also does not induce adult ovary defects. bab1-Gal4<sup>Pgal4-2</sup>, an additional Gal4 line active in both apical cells and terminal filaments at P0, does induce adult ovary defects based on loss of ovariole and sheath morphology. For each condition, the severity of the phenotype and the proportion of ovary pairs observed for that phenotype are indicated. See Fig. S3 for the activity of the drivers in P0 ovaries.



**Supplementary Figure 6. Efficacy of Engrailed and Invected knock down in developing ovaries and corresponding phenotypes.** Engrailed/Invected immunostaining of P0 ovaries demonstrating the efficacy of UAS- En and Inv dsRNA constructs in knocking down En/Inv expression when driven by Lmx1a-Gal4 (A). Corresponding adult ovary phenotypes are displayed below (B). The En<sup>RNAi</sup> GD35697 recombined with Inv<sup>RNAi</sup> reveals the most effective knock down and induces a mild phenotype. En/Inv knock down was further assessed using this recombinant, as displayed in figure 7.



**Supplementary Figure 7. Chip is required in the Lmx1a-Gal4 lineage of the ovary.** Three UAS-RNAi lines targeting two separate regions of the Chip transcript induce ovary defects when driven by the Lmx1a-Gal4 driver, as shown by loss of overall ovary material and ovariole morphology (nuclei, Hoechst, green) and sheath (F-actin stain, Phalloidin, magenta).



Supplementary Table 1. RNA sequencing analysis: Genes enriched in ovary-containing samples whose expression is affected in Lmx1a homozygous mutants.

Gene Name	Enrichment in Ovaries+FatBody samples versus FatBody in $\Delta 1/+$		$\Delta 1/\Delta 1$ versus $\Delta 1/+$ in Ovaries+FatBody samples	
	log2FoldChange	Padj	log2FoldChange	Padj
CG9518	2.01	2.63E-04	-3.71	2.53E-08
HGTX	3.85	3.41E-10	-3.25	4.36E-07
wb	0.26	1.27E-02	-3.03	2.65E-20
otp	3.79	1.20E-50	-2.98	7.31E-05
rt	4.47	1.32E-24	-2.43	1.22E-13
CG9492	3.87	5.53E-26	-2.41	4.48E-06
<b>en</b>	<b>0.17</b>	<b>3.79E-03</b>	<b>-2.28</b>	<b>4.63E-05</b>
CG15822	1.55	8.42E-09	-1.99	3.88E-04
ea	0.37	8.69E-03	-1.88	5.76E-03
CG34347	0.78	4.48E-05	-1.86	2.06E-04
CG18586	1.00	7.16E-03	-1.85	4.41E-02
rtet	0.27	1.37E-02	-1.83	2.41E-17
<b>inv</b>	<b>3.54</b>	<b>4.88E-11</b>	<b>-1.81</b>	<b>2.28E-03</b>
<b>hh</b>	<b>0.44</b>	<b>4.61E-05</b>	<b>-1.73</b>	<b>1.12E-08</b>
Nrt	2.84	3.23E-55	-1.69	1.51E-03
<b>Sox100B</b>	<b>1.34</b>	<b>1.50E-04</b>	<b>-1.58</b>	<b>7.64E-06</b>
CG10738	1.37	1.76E-05	-1.57	2.59E-06
hbs	2.86	1.13E-06	-1.56	4.23E-03
CG42260	1.57	4.59E-09	-1.54	6.22E-03
Mur89F	3.53	3.33E-15	-1.51	7.01E-04
CG12592	0.21	1.70E-02	-1.51	2.82E-02
Timp	2.75	3.19E-05	-1.38	2.98E-02
CG42346	0.29	2.26E-02	-1.29	6.40E-03
<b>Ser</b>	<b>2.53</b>	<b>4.88E-10</b>	<b>-1.29</b>	<b>2.28E-03</b>
RhoGAP100F	0.32	2.85E-03	-1.27	9.78E-06
form3	2.03	3.76E-04	-1.18	3.27E-02
CG32165	1.43	3.61E-03	-1.15	1.96E-03
dysc	3.44	1.99E-12	-1.11	3.07E-02
CG4415	2.10	2.71E-03	-1.09	3.76E-02
CG13928	4.64	1.02E-51	-1.06	3.20E-02
ko	4.13	8.30E-23	-0.96	4.19E-03
<b>stumps</b>	<b>1.96</b>	<b>1.23E-06</b>	<b>-0.92</b>	<b>2.70E-03</b>
rec	2.69	6.35E-08	-0.91	4.43E-03
wake	3.20	1.62E-36	-0.84	2.34E-03
CG6812	2.17	1.58E-05	-0.73	1.11E-03
<b>ptc</b>	<b>1.60</b>	<b>5.59E-04</b>	<b>-0.66</b>	<b>2.06E-03</b>
lme4	3.25	4.29E-13	-0.50	5.42E-03
Uch-L5	1.01	1.05E-02	-0.48	6.13E-06
janA	1.05	6.08E-04	-0.42	2.68E-03
PIG-S	0.55	1.06E-02	-0.39	2.20E-02
Cpsf73	4.58	2.29E-25	-0.39	1.07E-03
trsn	0.75	5.61E-07	-0.37	4.24E-03
dalao	0.29	4.13E-03	-0.33	1.58E-02
CG5641	4.60	5.92E-28	-0.30	2.78E-02
Hpr1	0.35	1.40E-03	-0.27	4.19E-02
Ge-1	5.83	7.36E-44	-0.27	1.43E-05
Ddx1	1.68	5.31E-04	-0.23	2.87E-02
w	3.78	2.20E-27	-0.21	8.91E-01
rdgC	3.40	4.07E-11	1.75	1.99E-08
Fas3	3.57	4.68E-18	1.54	2.11E-06
CG6293	2.32	1.72E-12	1.50	6.94E-05
CG4096	1.17	3.40E-02	1.43	1.59E-07
CG13032	3.87	1.48E-17	1.40	1.24E-02
Nlg1	0.35	9.35E-03	1.30	3.88E-04
Tollo	2.84	2.89E-34	1.28	6.71E-12
Shaw	1.49	6.16E-13	1.25	2.39E-07
CG9411	2.93	2.40E-09	1.18	5.28E-04
ab	0.36	2.96E-03	0.66	3.27E-02
Spc105R	0.54	1.93E-13	0.66	1.32E-02
CTCF	3.22	1.72E-20	0.52	3.14E-05
CG3967	1.62	3.88E-06	0.40	7.66E-03
Atu	2.83	8.61E-17	0.28	4.31E-02
Dref	0.37	4.43E-04	0.20	4.42E-02

Genes down-regulated  
in  $\Delta 1/\Delta 1$  ovariesGenes up-regulated  
in  $\Delta 1/\Delta 1$  ovaries

**Supplementary Table 2. Detailed genotypes of animals described in each figure.**

<b>Figure</b>	<b>Genotype</b>
1A	Lmx1a <sup>Δ1</sup> -dsRed /TM3-GFP Lmx1a <sup>Δ1</sup> -dsRed / Lmx1a <sup>Δ1</sup> -dsRed
1B	Lmx1a-Gal4/+ Lmx1a <sup>RNAi KK</sup> / + ; Lmx1a-Gal4/+ Lmx1a-Gal4/Lmx1a <sup>RNAi TRIP</sup> Lmx1a-Gal4/Lmx1a <sup>RNAi GD</sup>
1C	Lmx1a-Gal4 / UAS-mCD8-GFP
1D	Lmx1a-Gal4, UAS-mCD8-GFP, Lmx1a <sup>Δ1</sup> -dsRed / +
1E	Gtrace / + ; Lmx1a-Gal4
1F	Gtrace / + ; Lmx1a-Gal4
2A	Lmx1a <sup>Δ1</sup> -dsRed /TM3-GFP Lmx1a <sup>Δ1</sup> -dsRed / Lmx1a <sup>Δ1</sup> -dsRed
2B	Lmx1a <sup>Δ1</sup> -dsRed /TM3-GFP Lmx1a <sup>Δ1</sup> -dsRed / Lmx1a <sup>Δ1</sup> -dsRed Lmx1a <sup>Δ1</sup> -dsRed /Df(3L)ED4475 Lmx1a <sup>Δ1</sup> -dsRed /Df(3L)ED4483 Lmx1a <sup>Δ1</sup> -dsRed /Df(3L)BSC380
2C	Lmx1a <sup>Δ1</sup> -dsRed /TM3-GFP Lmx1a <sup>Δ1</sup> -dsRed / Lmx1a <sup>Δ1</sup> -dsRed
2D	Lmx1a <sup>Δ1</sup> -dsRed /TM3-GFP Lmx1a <sup>Δ1</sup> -dsRed / Lmx1a <sup>Δ1</sup> -dsRed
2E	Lmx1a <sup>Δ1</sup> -dsRed /TM3-GFP Lmx1a <sup>Δ1</sup> -dsRed / Lmx1a <sup>Δ1</sup> -dsRed
2F	Lmx1a <sup>Δ1</sup> -dsRed, Bab1 <sup>P</sup> -LacZ /TM3-GFP Lmx1a <sup>Δ1</sup> -dsRed, Bab1 <sup>P</sup> -LacZ / Lmx1a <sup>Δ1</sup> -dsRed
3A	Lmx1a <sup>Δ1</sup> -dsRed /+ Lmx1a <sup>Δ1</sup> -dsRed, Lmx1a-Gal4/+ Lmx1a <sup>Δ1</sup> -dsRed / Lmx1a <sup>Δ1</sup> -dsRed Lmx1a <sup>Δ1</sup> -dsRed, Lmx1a-Gal4/ Lmx1a <sup>Δ1</sup> -dsRed Lmx1a <sup>Δ1</sup> -dsRed / Lmx1a <sup>Δ1</sup> -dsRed, UAS-Lmx1a Lmx1a <sup>Δ1</sup> -dsRed / Lmx1a <sup>Δ1</sup> -dsRed, UAS-cLmx1b Lmx1a <sup>Δ1</sup> -dsRed, Lmx1a-Gal4/ Lmx1a <sup>Δ1</sup> -dsRed, UAS-Lmx1a Lmx1a <sup>Δ1</sup> -dsRed, Lmx1a-Gal4/ Lmx1a <sup>Δ1</sup> -dsRed, UAS-cLmx1b
3B,C	Gtrace/+ ; Lmx1a-Gal4/+ Lmx1a <sup>RNAi KK</sup> / + ; Lmx1a-Gal4/+ Lmx1a-Gal4/Lmx1a <sup>RNAi TRIP</sup> Lmx1a-Gal4/Lmx1a <sup>RNAi GD</sup> Gtrace/+ ; Bab-Gal4 <sup>Agal4-5</sup> /+ Lmx1a <sup>RNAi KK</sup> / + ; Bab-Gal4 <sup>Agal4-5</sup> /+

- Bab-Gal4<sup>Agal4-5</sup>/Lmx1a<sup>RNAi TRiP</sup>  
 Bab-Gal4<sup>Agal4-5</sup>/Lmx1a<sup>RNAi GD</sup>  
 Gtrace/+ ; dLmx1b<sup>GMR35G09</sup>-Gal4/+  
 Lmx1a<sup>RNAi KK</sup> / + ; dLmx1b-Gal4<sup>GMR35G09</sup> / +  
 dLmx1b-Gal4<sup>GMR35G09</sup>/Lmx1a<sup>RNAi TRiP</sup>
- 3D Lmx1a-Gal4/+  
 Lmx1a-Gal4/Lmx1a<sup>RNAi TRiP</sup>  
 Gtrace/+ ; Bab-Gal4<sup>Agal4-5</sup>/+  
 Bab-Gal4<sup>Agal4-5</sup>/Lmx1a<sup>RNAi TRiP</sup>
- 4A + / tub-Gal80<sup>ts</sup> ; Lmx1a-Gal4 / +  
 Lmx1a<sup>RNAi KK</sup> / tub-Gal80<sup>ts</sup> ; Lmx1a-Gal4 / +
- 4B + / tub-Gal80<sup>ts</sup> ; Lmx1a-Gal4, Lmx1a<sup>Δ1</sup>-dsRed / +  
 + / tub-Gal80<sup>ts</sup> ; Lmx1a-Gal4, Lmx1a<sup>Δ1</sup>-dsRed / Lmx1a<sup>Δ1</sup>-dsRed  
 + / tub-Gal80<sup>ts</sup> ; Lmx1a-Gal4, Lmx1a<sup>Δ1</sup>-dsRed / Lmx1a<sup>Δ1</sup>-dsRed, UAS-Lmx1a
- 5A-D Lmx1a<sup>Δ1</sup>-dsRed / TM3-GFP  
 Lmx1a<sup>Δ1</sup>-dsRed / Lmx1a<sup>Δ1</sup>-dsRed
- 6A Lmx1a-Gal4, Bab1<sup>P</sup>-LacZ / +  
 Lmx1a-Gal4, Bab1<sup>P</sup>-LacZ / Lmx1a<sup>RNAi KK</sup>  
 Lmx1a-Gal4, Bab1<sup>P</sup>-LacZ / Lmx1a<sup>RNAi TRiP</sup>
- 6B Lmx1a-Gal4 / +  
 Lmx1a-Gal4 / Bab1<sup>RNAi 57410</sup>  
 Lmx1a-Gal4 / Bab1<sup>RNAi 49042</sup>
- 6C Bab1<sup>P</sup>-LacZ / +  
 Bab1<sup>P</sup>-LacZ / Bab1<sup>P</sup>-LacZ
- 7A Lmx1a-Gal4 / +  
 Lmx1a-Gal4 / Hh<sup>RNAi TRiP 25794</sup>  
 Sox100B<sup>RNAi TRiP 57417</sup> / + ; Lmx1a-Gal4 / +  
 Lmx1a-Gal4 / Invested<sup>RNAi TRiP 41675</sup>, Engrailed<sup>RNAi GD 35697</sup>
- 7B Lmx1a-Gal4, Bab1<sup>P</sup>-LacZ / +  
 Lmx1a-Gal4, Bab1<sup>P</sup>-LacZ / Hh<sup>RNAi TRiP 25794</sup>  
 Sox100B<sup>RNAi TRiP 57417</sup> / + ; Lmx1a-Gal4, Bab1<sup>P</sup>-LacZ / +  
 Lmx1a-Gal4, Bab1<sup>P</sup>-LacZ / Invested<sup>RNAi TRiP 41675</sup>, Engrailed<sup>RNAi GD 35697</sup>
- S1C W<sup>1118</sup>  
 Lmx1a<sup>Δ1</sup>-dsRed / Lmx1a<sup>Δ1</sup>-dsRed
- S1D W<sup>1118</sup>  
 Lmx1a<sup>Δ1</sup>-dsRed / Lmx1a<sup>Δ1</sup>-dsRed
- S1E Gtrace/+ ; Lmx1a-Gal4/+  
 Lmx1a<sup>RNAi KK</sup> / + ; Lmx1a-Gal4/+  
 Lmx1a-Gal4/Lmx1a<sup>RNAi GD</sup>  
 Lmx1a-Gal4/Lmx1a<sup>RNAi TRiP</sup>
- S1F Lmx1a-Gal4, UAS-mCD8-GFP, Lmx1a<sup>Δ1</sup>-dsRed / +
- S2A Lmx1a<sup>Δ1</sup>-dsRed / TM3-GFP

	Lmx1a <sup>Δ1</sup> -dsRed / Lmx1aΔ1-dsRed
S2B	Lmx1a <sup>Δ1</sup> -dsRed (non-isogenic) / TM3 Lmx1a <sup>Δ1</sup> -dsRed (non-isogenic) / Lmx1aΔ1-dsRed (non-isogenic)
S2C	Vkg-GFP, Lmx1a <sup>Δ1</sup> -dsRed / TM3-GFP Vkg-GFP, Lmx1a <sup>Δ1</sup> -dsRed / Lmx1a <sup>Δ1</sup> -dsRed
S3A	w ; GMR-Gal4 , UAS-GFP / + w ; GMR-Gal4 , UAS-GFP / + ; UAS-Lmx1a-HA
S3B	Lmx1a <sup>Δ1</sup> -dsRed / + Lmx1a <sup>Δ1</sup> -dsRed, Lmx1a-Gal4/+ Lmx1a <sup>Δ1</sup> -dsRed / Lmx1a <sup>Δ1</sup> -dsRed Lmx1a <sup>Δ1</sup> -dsRed, Lmx1a-Gal4/ Lmx1a <sup>Δ1</sup> -dsRed Lmx1a <sup>Δ1</sup> -dsRed / Lmx1a <sup>Δ1</sup> -dsRed, UAS-Lmx1a Lmx1a <sup>Δ1</sup> -dsRed / Lmx1a <sup>Δ1</sup> -dsRed, UAS-cLmx1b Lmx1a <sup>Δ1</sup> -dsRed, Lmx1a-Gal4/ Lmx1a <sup>Δ1</sup> -dsRed, UAS-Lmx1a Lmx1a <sup>Δ1</sup> -dsRed, Lmx1a-Gal4/ Lmx1a <sup>Δ1</sup> -dsRed, UAS-cLmx1b
S4	Gtrace ; Lmx1a-Gal4/+ Gtrace ; Bab1-Gal4 <sup>Agal4-5</sup> Gtrace ; dLmx1b-Gal4 <sup>GMR35G09</sup> Gtrace ; htl-Gal4 <sup>BL40669</sup> Gtrace ; ths-Gal4 <sup>BL47051</sup>
S5	Gtrace ; ths-Gal4 <sup>BL47051</sup> ths-Gal4 <sup>BL47051</sup> / Lmx1a <sup>RNAi GD</sup> ths-Gal4 <sup>BL47051</sup> / Lmx1a <sup>RNAi TRIP</sup> Lmx1a <sup>RNAi KK</sup> / + ; ths-Gal4 <sup>BL47051</sup> / + Gtrace ; htl-Gal4 <sup>BL40669</sup> htl-Gal4 <sup>BL40669</sup> / Lmx1a <sup>RNAi GD</sup> htl-Gal4 <sup>BL40669</sup> / Lmx1a <sup>RNAi TRIP</sup> Lmx1a <sup>RNAi KK</sup> / + ; htl-Gal4 <sup>BL40669</sup> / + Gtrace ; Bab1-Gal4 <sup>Agal4-2</sup> Lmx1a <sup>RNAi KK</sup> / + ; bab1-Gal4 <sup>Pgal4-2</sup> / +
S6	Lmx1a-Gal4, Bab1 <sup>P</sup> -LacZ / + Lmx1a-Gal4 Bab1 <sup>P</sup> -LacZ / + ; Engrailed <sup>RNAi GD 35697</sup> / + Lmx1a-Gal4 Bab1 <sup>P</sup> -LacZ / + ; Engrailed <sup>RNAi GD 35698</sup> / + Lmx1a-Gal4 Bab1 <sup>P</sup> -LacZ / + ; Invected <sup>RNAi TRIP 41675</sup> / + Lmx1a-Gal4 Bab1 <sup>P</sup> -LacZ / + ; Invected <sup>RNAi TRIP 41675</sup> , Engrailed <sup>RNAi GD 35697</sup> / + Lmx1a-Gal4 Bab1 <sup>P</sup> -LacZ / + ; Invected <sup>RNAi TRIP 41675</sup> , Engrailed <sup>RNAi GD 35698</sup> / + Lmx1a-Gal4 / + Lmx1a-Gal4 / + ; Engrailed <sup>RNAi GD 35697</sup> / + Lmx1a-Gal4 / + ; Engrailed <sup>RNAi GD 35698</sup> / + Lmx1a-Gal4 / + ; Invected <sup>RNAi TRIP 41675</sup> / + Lmx1a-Gal4 / + ; Invected <sup>RNAi TRIP 41675</sup> , Engrailed <sup>RNAi GD 35697</sup> / +

Lmx1a-Gal4 / + ; Invected<sup>RNAi TRiP</sup> 41675, Engrailed<sup>RNAi GD 35698</sup> / +

S7

Lmx1a-Gal4 / +  
Chip<sup>RNAi KK</sup> / + ; Lmx1a-Gal4 / +  
Lmx1a-Gal4 / Chip<sup>RNAi TRiP</sup>  
Chip<sup>RNAi GD</sup> / + ; Lmx1a-Gal4 / +**Supplementary Table 3. Oligonucleotide primers used in this study.**

	Forward	Reverse
<b>qPCR primers</b>		
Actin5c	5'-CTCGCCACTTGC GTTTACAGT-3'	5'-TCCATATCGTCCC ACTTTGGTC-3'
Lmx1a/CG32105	5'-CAGTAGCCACCTCGCAATTA-3'	5'-CGAAGTTCTTCTCGCACTTGA-3'
Vasa	5'-CGGTCTGGCTGTACGAAA-3'	5'-CCCTCTTTCACCACGTTCA-3'
Fbp2	5'-TCGACAAGGATGTGGAGACTA-3'	5'-CAGAGGACATGTTAACCACCAT-3'
bab1	5'-CGAGATGATCCGAGAGGAAG-3'	5'-GGTTGGTGTCCAGCACTTT-3'
bab2	5'-GGAGATCAAGCCAGAAATCG-3'	5'-TCTGCTGATTGGTGTCCAG-3'
Hh	5'-CCACATCTACTGCTCCGTC A -3'	5'-GTTTTGCATCTGCTCGAGGT-3'
Ser	5'-TGCCTGCAACTTAATTGCTTT-3'	5'-CTATCGTCTTGGTGGCCCTAAG-3'
<b>Lmx1a<math>\Delta</math>1-dsRed mutant</b>		
Lmx1a <sup><math>\Delta</math>1</sup> -dsRed genotyping	5'-CTCCCACAACGAGGACTACA-3'	5'-GCTGAGCTGCCATCTGTTAAT-3'
Lmx1a gRNA	5'-CTTCGATTTGCTGAGGCCACGGGA-3' (sense)	5'-AAACTCCCGTGGCCTCAGCAAATC-3' (antisense)
HDR 5' Homology Arm	5'-AAGAATTCCTGCCTCTACTGCTGCCACTGC-3'	5'-AAGCGGCCGCTCGTATACGAGTTGCCACA-3'
HDR 3' Homology Arm	5'-AAACTAGTGATGGCCATTGGCTGGAATG-3'	5'-AACTCGAGTTGGTTCGAGTTTCATAAAAGC-3'